Dendritic Iron Porphyrins with Tethered Axial Ligands: New Model Compounds for Cytochromes

by **Philipp Weyermann** and **François Diederich***

Laboratorium für Organische Chemie, ETH-Hönggerberg, HCI, CH-8093 Zürich

and

Jean-Paul Gisselbrecht, **Corinne Boudon**, and **Maurice Gross**

Laboratoire d'Electrochimie et de Chimie Physique du Corps Solide, Université Louis Pasteur and CNRS, UMR No. 7512, 4, rue Blaise Pascal, F-67000 Strasbourg

The novel dendritic iron porphyrins of generation zero ([**1**·Fe^{III}]Cl), one ([**2**·Fe^{III}]Cl), and two ([**3**·Fe^{III}]Cl) (*Fig. 1*) were prepared as models of cytochromes (*Schemes 1* and *2*). They feature controlled axial ligation at the iron center by two imidazoles tethered to the porphyrin core. Similar to the core compound [**4**·Fe^{III}]Cl, they are six-coordinate low-spin complexes as demonstrated by UV/VIS (*Figs. 3* and *4*) and EPR spectroscopy, as well as measurements of the magnetic moments by the *Evans-Scheffold* method. The coordination environment does not change upon reduction to the corresponding iron(II) complexes. The dendritic iron porphyrins were purified by size-exclusion chromatography and shown by matrix-assisted laser-desorption-ionization mass spectrometry (MALDI-TOF-MS; *Figs. 5* and *6*) to be free of structural defects. With their triethyleneglycol monomethyl ether surface groups, the three dendritic mimics are soluble in solvents of widely differing polarity. Electrochemical studies (*Figs. 7* and *8*) and optical redox titrations (*Fig. 9*) revealed that the potential of the Fe^{III}/Fe^{II} couple in CH_2Cl_2, MeCN, and H_2O shifts strongly to more positive values (by as much as 380 mV) with increasing dendritic generation (*Fig. 10*). The redox potential of the second-generation complex [**3**·Fe^{III}]Cl is, within experimental error, identical in all three solvents, which clearly demonstrates that the dendritic branching creates a unique local microenvironment around the isolated electroactive core. Whereas, in the organic solvents, the largest anodic potential shift is measured upon changing from generation zero to one, the largest shift in H_2O occurs only at the level of the second generation, when the dendritic superstructure is sufficiently dense to prevent access of bulk solvent to the electroactive core.

1. Introduction. – The most intriguing characteristics of the cytochrome family of electron-transfer proteins is the very broad range of redox potentials featured by the Fe^{III}/Fe^{II} couple at the electroactive heme core [1]. A variety of model studies have identified a dependency of this potential from the nature of substituents at the porphyrin ring [2], axial ligation to the iron center [3], H-bonding to the axial ligands [4], and ruffling of the porphyrin macrocycle [5]. In contrast, the influence of environmental effects such as heme solvation [6], polarity of the heme microenvironment [7], and the nature of the surrounding protein shell [8] have not been intensively investigated with model compounds and are less well-understood.

We have already reported the use of dendritic iron porphyrins [9] as model compounds for cytochromes in which the protein shell around the buried electroactive core is mimicked by the dendritic superstructure (for other dendritic porphyrins and reviews on electroactive dendrimers, see [10][11]). These investigations revealed a strong correlation between the redox potential of the Fe^{III}/Fe^{II} couple and the degree of dendritic branching. In these earlier systems, however, the nature of the axial ligation to

the Fe center, which is known to have a very strong influence on the redox properties [3], was not controlled. Therefore, the observed potential shifts caused by the dendritic shell could not be quantified independently from axial ligation effects, and no general conclusions concerning the effects of the dendritic superstructure could be drawn.

We now present a new series of dendritic cytochrome mimics that contain a defined and stable axial ligation pattern. This allows, for the first time, a quantitative evaluation of the effect of an insulating dendritic shell on the redox properties of the embedded iron porphyrin core (for a preliminary communication of parts of this work, see [12]).

The three novel dendrimers of generation zero ([**1**·Fe^{III}]Cl), one ([**2**·Fe^{III}]Cl), and two ([**3**·Fe^{III}]Cl) (*Fig. 1*) feature controlled axial ligation at the iron center by two imidazoles tethered to the porphyrin core. This thermodynamically stable ligation pattern, which is kinetically inert towards coordinating solvents, is found in the cytochrome-b_5 family of electron-transfer proteins [13]. The optimal length of the alkyl tethers between the Fe-coordinating imidazoles and the *meso*-phenyl ring at the porphyrin core was selected with the help of molecular modeling [14]. The modeling predicted that tethers consisting of five or more CH_2 units would allow nearly strain-free intramolecular ligation of the imidazole at the Fe center. A tether length of six rather than five CH_2 units was chosen to allow a certain conformational flexibility after coordination. The second-generation compound in this new series, ([**3**·Fe^{III}]Cl; M_r 11719 Da), is comparable in mass and size (*Fig. 2*) to typical single-heme cytochromes such as *Bonita* (tuna) cytochrome-*c* (M_r 11384 Da) [15], or bovine cytochrome-b_5 (M_r 15198 Da) [13]. With their triethyleneglycol-monomethyl-ether surface groups, all three dendritic mimics are freely soluble in common organic solvents and in H_2O, which allowed comparative investigations in environments of different polarity, as well as under biologically relevant aqueous conditions.

2. Results. – 2.1. *Synthesis and Characterization of the Porphyrin Core.* The key intermediate in the synthesis of the dendritic porphyrins was the bis-imidazole-appended zinc porphyrin **4**·Zn, which was prepared in high yield by a *Suzuki* cross-coupling [16] between the brominated zinc porphyrin **5**·Zn and the bis-imidazole-appended phenylboronic ester **6** (*Scheme 1*). The *meso*-bromoporphyrin **5**·Zn was obtained from precursor **7**·2 H [9c] by dibromination with *N*-bromosuccinimide (NBS) in $CHCl_3$ to give *meso*-dibromoporphyrin **8**·2 H and partial reduction with Bu_3SnH in PhH to give monobromoporphyrin **5**·2 H, after chromatographic separation from by-product **7**·2 H and residual starting material. Metallation of the free-base porphyrin was then carried out with $Zn(OAc)_2 \cdot 2\ H_2O$ in $CHCl_3$/MeOH. This sequence of reactions provided regioisomerically pure **5**·Zn, since the intermediate dibromo derivative **8**·2 H could be purified to isomeric homogeneity by chromatography on SiO_2. In contrast, direct monobromination of **7**·2 H with NBS in $CHCl_3$ led, in addition to **8**·2 H as a by-product and leftover starting material, to a mixture of isomeric monobrominated compounds (up to 15% bromination at β-positions), which, in our hands, were impossible to separate by chromatographic methods. Phenylboronate **6** was prepared from 4-bromo-2,6-dimethoxytoluene (**9**) [17] by cleavage of the methyl-ether groups with HI ($\rightarrow$**10**), reprotection of the phenolic OH groups with chloromethyl methyl ether (MOM-Cl; $\rightarrow$**11**), metallation with BuLi and boronate formation with $B(OMe)_3$ and pinacol ($\rightarrow$**12**), cleavage of the MOM protecting groups

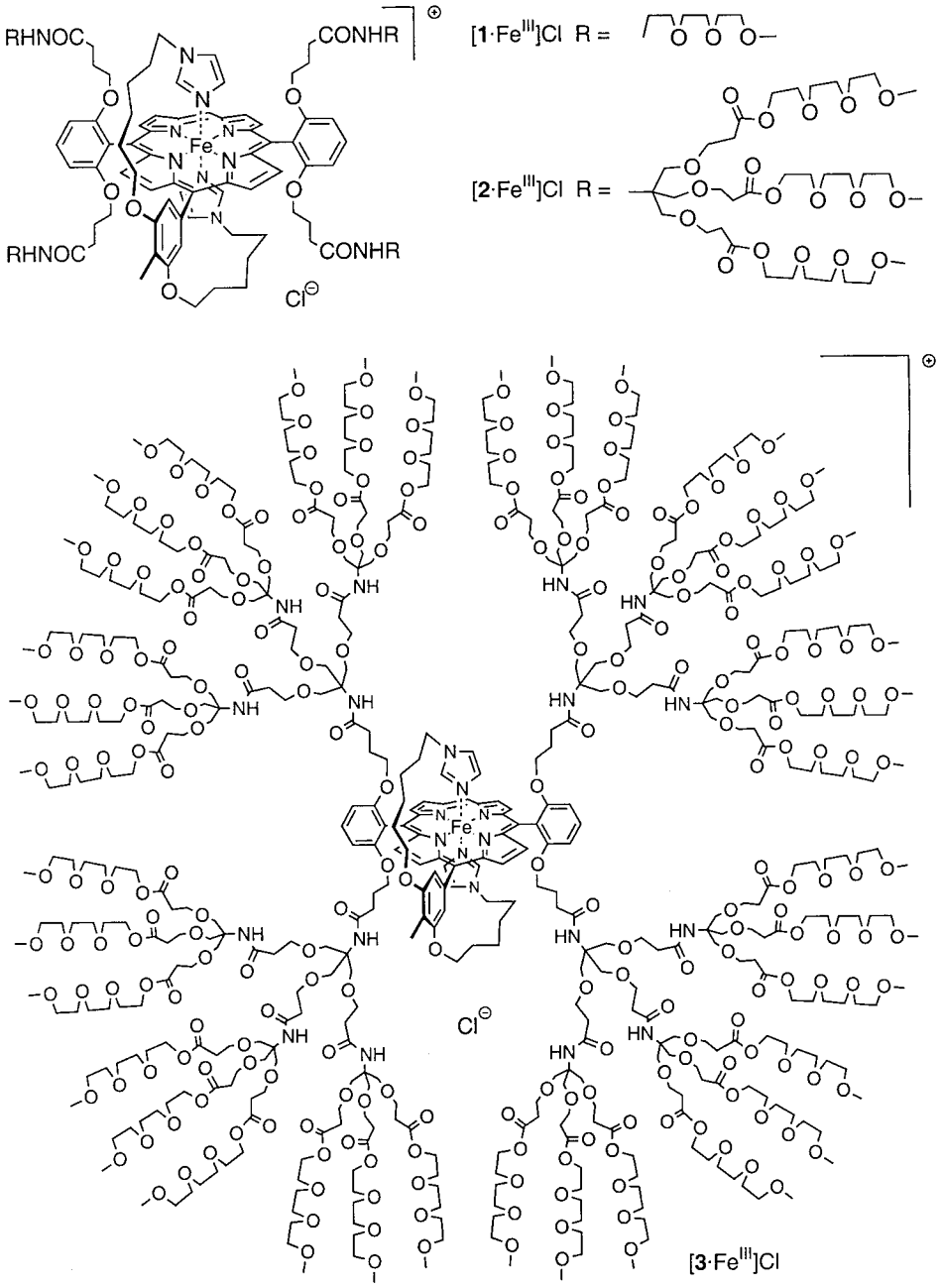

Fig. 1. *Dendritic iron porphyrins [**1** · Fe^{III}]Cl, [**2** · Fe^{III}]Cl, and [**3** · Fe^{III}]Cl with defined axial ligation as models for cytochromes*

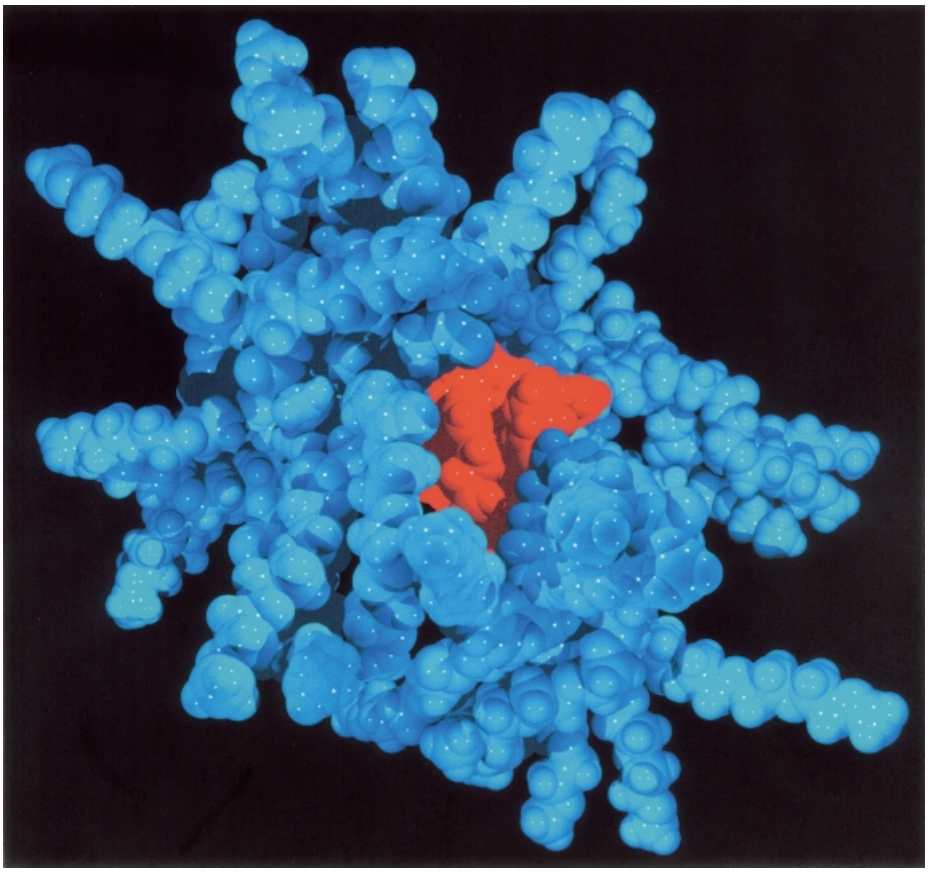

Fig. 2. *Space-filling representation of the second-generation dendritic iron porphyrin [**3**·Fe^{III}]Cl showing the almost complete encapsulation of the porphyrin core by the dendritic shell.* The average diameter of the roughly spherical molecule is 4.5 Å.

with HCl (→ **13**), and alkylation with 1-(6-bromohexyl)imidazole (**14**) (its hydrochloride salt has been reported, see [18]).

Omission of the deprotection/reprotection procedure led to complete decomposition of the boronate moiety in all attempts to achieve cleavage of the methyl ether to free OH groups. Installation of the boronate moiety at a later stage in the sequence after introduction of the imidazole moieties by Pd^0-catalyzed cross-coupling methodology was unsuccessful. This result was probably due to coordinating interference of the imidazole ligands in the catalytic cycle of the reaction. However, the critical *Suzuki* cross-coupling between **6** and bromoporphyrin **5**·Zn, albeit Pd^0-catalyzed as well, was very efficient and provided the desired product **4**·Zn in 82% yield. The use of Cs_2CO_3 as a base was important to achieve high yields, whereas the solvent mixture (PhMe/THF) for the cross-coupling was chosen mainly because of the good solubility for **6**, which considerably sped up the reaction compared to either solvent used neat.

Scheme 1. *Synthesis of the Bis-Imidazole-Ligated Iron(III) Porphyrin Core [**4**·Fe^{III}]Cl*

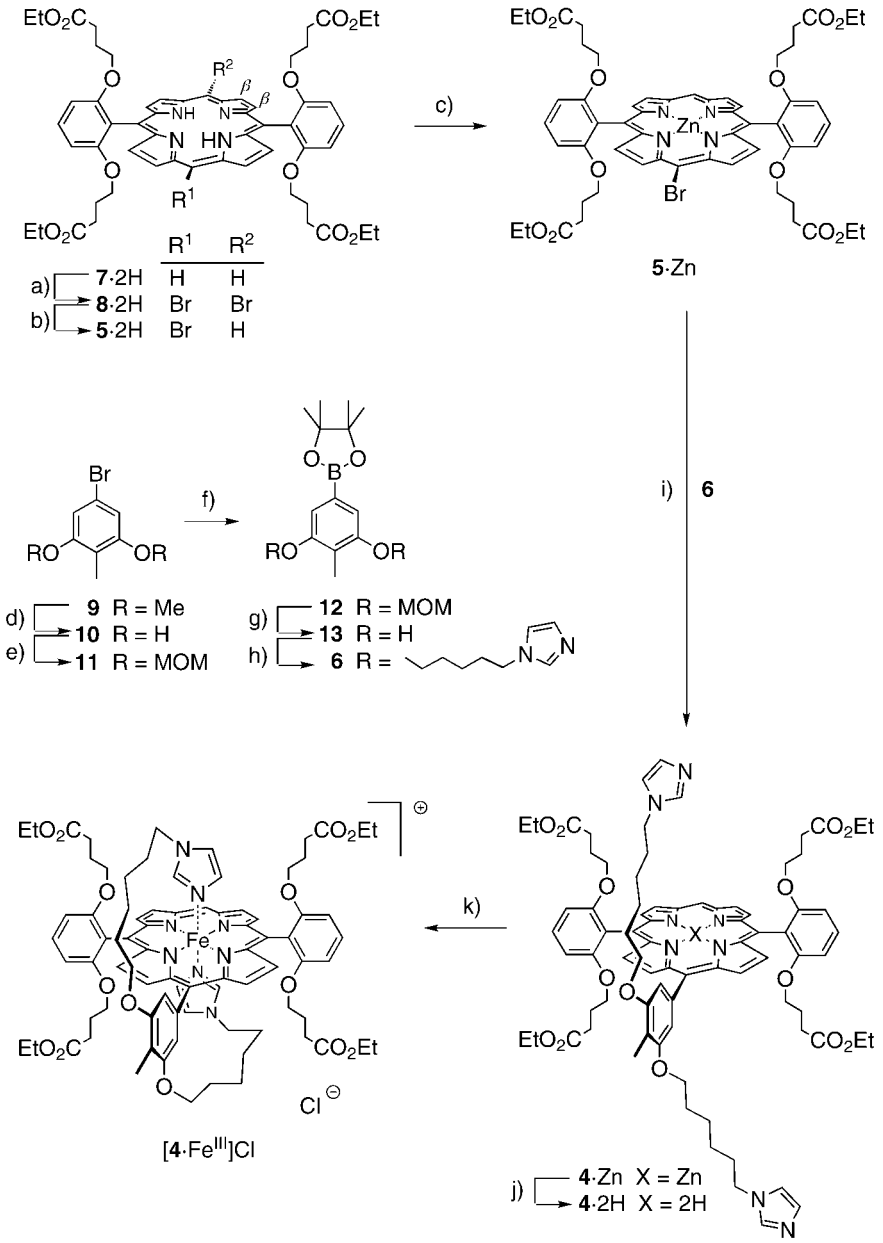

a) NBS, $CHCl_3$, r.t., 30 min; 91%. *b*) Bu_3SnH, AIBN, PhH, reflux, 2 h; 43%. *c*) $Zn(OAc)_2 \cdot 2\,H_2O$, $CHCl_3$/MeOH, r.t., 1 h; 78%. *d*) HI, AcOH, reflux, 6 h; 94%. *e*) MOM-Cl, K_2CO_3, MeCN, 0°, 30 min; 96%. *f*) BuLi, TMEDA, THF, −78°, 1 h, then $B(OMe)_3$, −78° → r.t., 3 h, then pinacol, PhH, reflux, 12 h; 97%. *g*) Conc. aq. HCl soln., THF/MeOH, r.t., 3 d; 51%. *h*) 1-(6-Bromohexyl)imidazole (**14**), Cs_2CO_3, DMF, r.t., 16 h; 49%. *i*) **6**, [$Pd(PPh_3)_4$], Cs_2CO_3, PhMe/THF, reflux, 6 h; 82%. *j*) CF_3COOH, $CHCl_3$, r.t., 10 min; 78%. *k*) $FeCl_2$, 2,6-lutidine, THF, reflux, 2 h; then air; then 1% HCl in $CHCl_3$, r.t., 5 min; then 'proton sponge', THF, r.t., 15 min; 65%. NBS = *N*-bromosuccinimide; AIBN = α,α'-azobis[isobutyronitrile]; MOM = methoxymethyl; TMEDA = *N,N,N′,N′*-tetramethylethylenediamine; 'proton sponge' = 1,8-bis(dimethylamino)naphthalene.

^{1}H-NMR Spectroscopy in $CDCl_3$ showed that **4**·Zn exists as a dynamic, five-coordinate complex, with both imidazole ligands switching between complexed and free states, which led to strong signal broadening and a large upfield shift of the aromatic proton resonances of the two appended ligands. These were observed as severely broadened *singlets* at 3.21 ppm (2 H) and 5.88 ppm (1 H), due to their positioning above the shielding anisotropic region of the porphyrin macrocycle, forced by their coordination to the metal center. When ^{1}H-NMR measurements were carried out in (D_5)pyridine, which, at the concentration present, efficiently displaces the intramolecular ligands from the metal center, all resonances were sharp, and the signals of the imidazole protons were observed at their expected positions at 7.10, 7.24, and 7.70 ppm, thus confirming the conclusions drawn above regarding intramolecular coordination.

The Fe^{III} complex [**4**·Fe^{III}]Cl was obtained from **4**·Zn by CF_3COOH-induced demetallation ($\rightarrow$**4**·2 H) and subsequent insertion of Fe^{II} by treatment with $FeCl_2$, followed by air oxidation. To ensure a homogeneous, oxygen-free coordination sphere after autoxidation and chromatography on neutral alumina, an acidic workup step with HCl in $CHCl_3$, leading to complete displacement of any present axial ligands by chloride, was carried out. This was followed by inducing recomplexation of the internal imidazoles *via* treatment with a strong, noncoordinating base ('proton sponge' = 1,8-bis(dimethylamino)naphthalene) [3c]. Care was taken to exclude the presence of H_2O during this entire workup, to prevent the formation of hydroxy complexes under the basic conditions of the last step. A model compound of very similar coordination environment, [**7**·Fe^{III}(*N*-MeIm)$_2$]Cl, with two *N*-methylimidazole (*N*-MeIm) molecules as axial ligands, was prepared by iron insertion into **7**·2 H under identical conditions followed by simple addition of excess *N*-MeIm.

Comparison of the Fe^{III} complex [**4**·Fe^{III}]Cl with the six-coordinate Fe^{III} model complex [**7**·Fe^{III}(*N*-MeIm)$_2$]Cl unambiguously showed complete intramolecular axial coordination of the two tethered imidazoles under formation of a paramagnetic low-spin complex. The UV/VIS [19] and EPR spectra [20] as well as the magnetic moments [21], determined by the *Evans-Scheffold* method [22], of both compounds compared very well with those of other bis-imidazole-coordinated Fe^{III} porphyrins. Reduction of [**4**·Fe^{III}]Cl, similar to [**7**·Fe^{III}(*N*-MeIm)$_2$]Cl, with $Na_2S_2O_4$ produced a diamagnetic low-spin complex with a hemochrome absorption spectrum, which was readily identified as that of a six-coordinate Fe^{II} species [23]. These Fe^{II} species were, as expected, very sensitive towards O_2, and re-oxidized without other decomposition to the Fe^{III} forms within seconds, when exposed to the atmosphere. The striking similarity in the behavior of [**4**·Fe^{III}]Cl and the model compound [**7**·Fe^{III}(*N*-MeIm)$_2$]Cl is visualized in *Figs. 3* and *4*, which depict UV/VIS spectra of the two compounds under four sets of different conditions.

In the oxidized Fe^{III} form at neutral pH, both compounds exist as six-coordinate, low-spin bis-imidazole complexes (*Figs. 3* and *4*), as confirmed by their UV/VIS properties [19] and their magnetic moments of $2.19 \pm 0.05\ \mu_B$ ([**4**·Fe^{III}]Cl) and $2.05 \pm 0.05\ \mu_B$ ([**7**·Fe^{III}(*N*-MeIm)$_2$]Cl) [21], which indicate one unpaired electron. Also, the rhombic EPR spectrum is characteristic of such compounds [20]. At acidic pH, the corresponding five-coordinate, high-spin chloride complexes are present in solution. These are identified by their characteristic UV/VIS spectra [19] and axial EPR signals

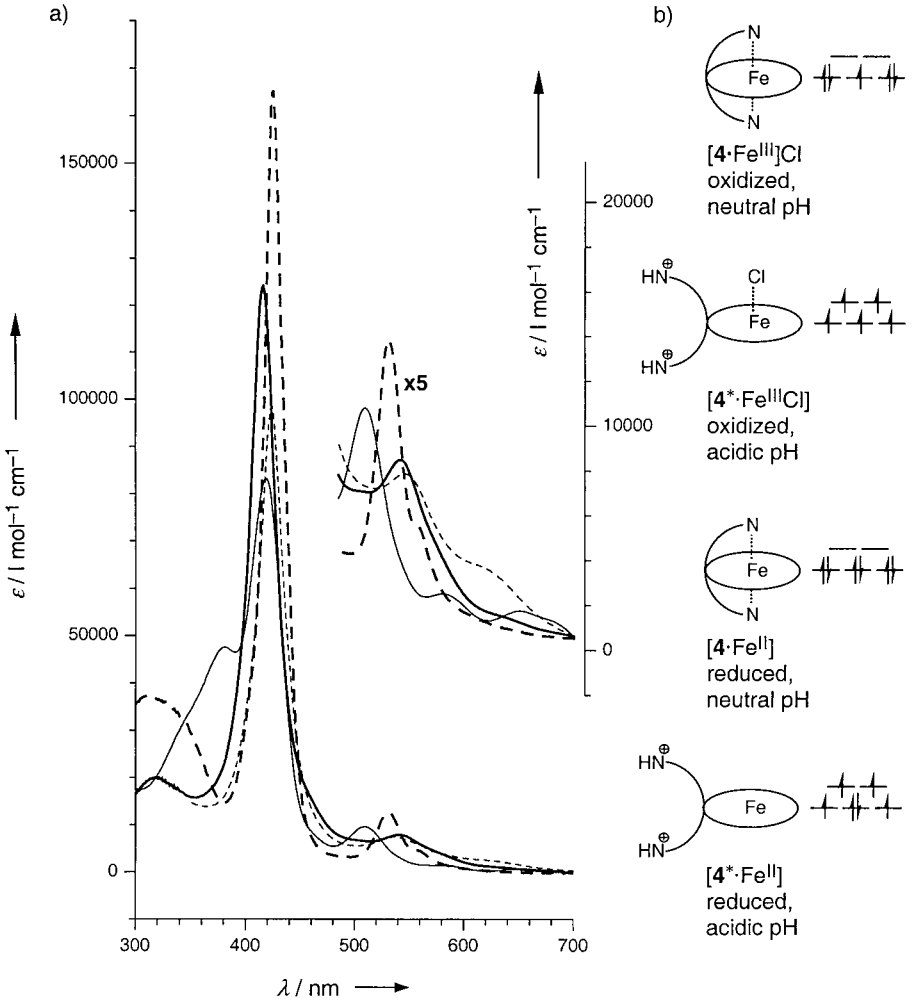

Fig. 3. a) *UV/VIS Spectra of [4 · Fe^{III}]Cl in $CHCl_3$ at room temperature in oxidized and reduced forms at neutral and acidic pH.* ——: [**4** · Fe^{III}]Cl, – – – –: [**4** · Fe^{II}], ——: [**4*** · Fe^{III}Cl], - - - - -: [**4*** · Fe^{II}]. b) *Schematic illustration of coordination environments and spin-states of the various species in the approximation of an octahedral crystal field* (* = tethered imidazoles both protonated).

[20], as well as by their magnetic moments of $5.85 \pm 0.05\ \mu_B$ ([**4*** · Fe^{III}Cl], with the two tethered imidazole moieties both protonated) and $5.79 \pm 0.05\ \mu_B$ ([**7** · Fe^{III}Cl]) [21], indicating five unpaired electrons. In the reduced Fe^{II} form at neutral pH, both compounds exist as six-coordinate, low-spin bis-imidazole complexes ([**4** · Fe^{II}] and [**7** · Fe^{II}(*N*-MeIm)$_2$]), evident from their very characteristic hemochrome spectra in the UV/VIS region [23] and their experimentally confirmed diamagnetism. The corresponding four-coordinate, high-spin complexes with no axial ligands present, [**4*** · Fe^{II}] and [**7** · Fe^{II}], which presumably prevail at acidic pH, were not studied with any method other than UV/VIS spectroscopy.

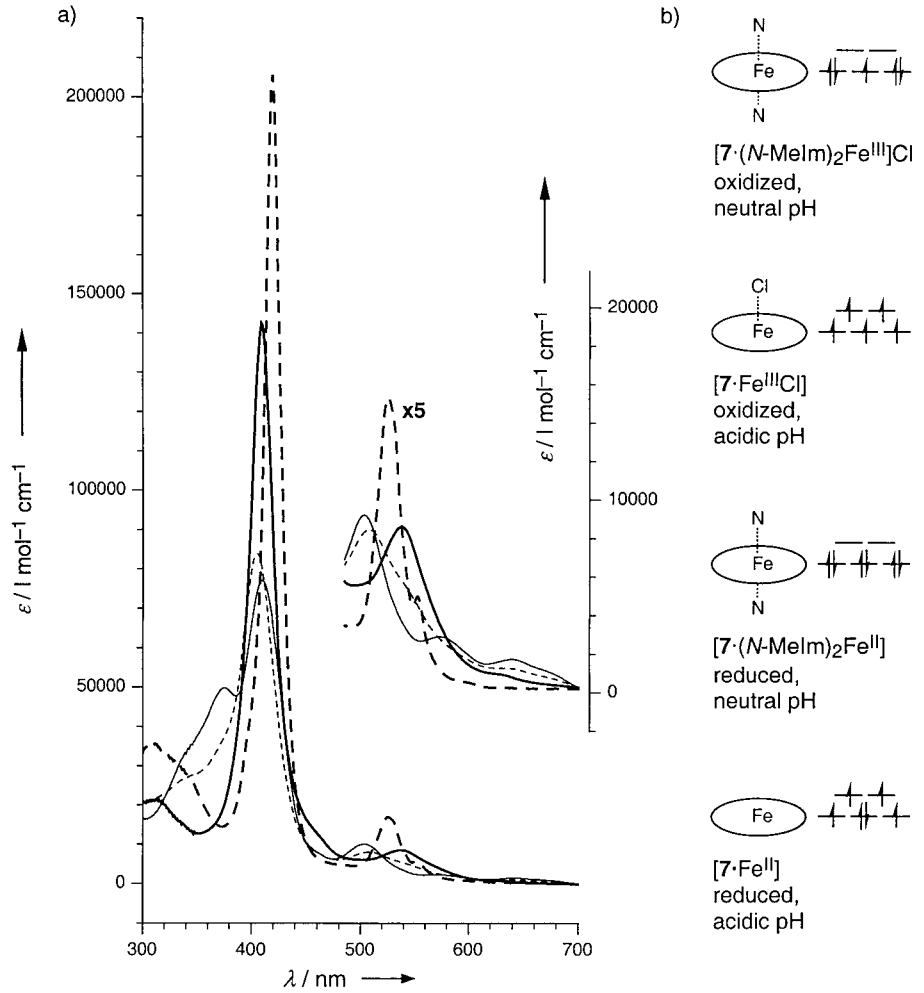

Fig. 4. a) *UV/VIS Spectra of model compound [7 · (N-MeIm)$_2$Fe^{III}]Cl in CHCl$_3$ at room temperature in oxidized and reduced form at neutral and acidic pH.* ——: [**7** · (*N*-MeIm)$_2$Fe^{III}]Cl, – – – –: [**7** · (*N*-MeIm)$_2$Fe^{II}], ——: [**7** · Fe^{III}Cl], - - - - -: [**7** · Fe^{II}]. b) *Schematic illustration of coordination environments and spin-states of the various species in the approximation of an octahedral crystal field.*

The detailed, comparative physico-chemical characterization of the new porphyrin core [**4** · Fe^{III}]Cl and model compound [**7** · Fe^{III}(*N*-MeIm)$_2$]Cl, which possesses a defined bis-imidazole axial ligation pattern, as well as comparisons with similar, well-characterized compounds known from the literature, establishes beyond any doubt the complete internal coordination of the two imidazoles to the iron metal center in [**4** · Fe^{III}]Cl. In addition, it was shown that the coordination environment does not change upon reduction to [**4** · Fe^{II}], which was a crucial point for the planned electrochemical experiments.

2.2. *Synthesis and Characterization of the Dendritic Porphyrins.* With the required porphyrin core in hand, the synthesis of dendrimers was addressed next. In contrast to our earlier work [9], in which divergent strategies had been applied to synthesize porphyrin dendrimers, we envisaged following a convergent dendrimer synthesis for the present study, to ensure highest structural homogeneity and absence of defects in the dendritic shell. For the preparation of the dendritic zinc porphyrins of generation zero (**1**·Zn), one (**2**·Zn), and two (**3**·Zn), the core tetraacid **15**·Zn, obtained by hydrolysis of **4**·Zn, was coupled to the corresponding dendritic wedges **16** [24], **17** [25], and **18**, respectively, with HATU (HATU = *O*-(7-azabenzotriazol-1-yl)-*N,N,N′,N′*-tetramethyluronium hexafluorophosphate) as the coupling reagent (*Scheme 2*). DMF was employed as solvent for this reaction, because tetraacid **15**·Zn showed very poor solubility in all other solvents except Me_2SO and basic H_2O. The second-generation dendritic wedge **18** was prepared from **17**, and triacid **19** *via* **20**, in analogy to the synthesis of similar dendrons with a glycine spacer attached to the focal point [25]. Porphyrin dendrimers **1**·Zn and **2**·Zn were readily purified by preparative gel-permeation chromatography (GPC; *Bio-Rad Bio-Beads S-X1*; CH_2Cl_2), but the isolation of pure **3**·Zn required the combined use of preparative GPC (*Bio-Rad Bio-Beads S-X1*; CH_2Cl_2) and high-performance gel-permeation chromatography (HP-GPC, *NovoGROM* 100 beads; THF). A significant decrease in dendrimer yield was observed with increasing steric bulk of the dendritic wedges: whereas **1**·Zn was isolated in 85% yield (starting from **4**·Zn), **2**·Zn was obtained in 65% and **3**·Zn in only 42% yield. This trend reflects both decreased coupling efficiency, as well as increasingly demanding purification problems. However, for a convergent dendrimer synthesis with a dendritic wedge of the size of **18**, the yield of **3**·Zn is still quite acceptable.

All three compounds were fully characterized by standard spectroscopic methods. In these Zn^{II}-porphyrin derivatives, again only one imidazole is complexed to the metal ion, forming a dynamic five-coordinate species. This led to severe line broadening, even more so than in case of the core **4**·Zn, and noninterpretable ^1H- and ^{13}C-NMR spectra resulted, when $CDCl_3$ was used as a solvent. NMR characterization was therefore performed in (D_5)pyridine, in which nearly all ^1H and ^{13}C resonances, in particular the characteristic signals of the porphyrin macrocycle, could be well-observed. Dendritic purity and homogeneity were best evidenced by MALDI-TOF-MS, which, in all cases, showed the strong molecular ion peak ($[M + Na]^+$) as the only major signal (*Fig. 5*). The agreement between calculated and measured positions of the maxima within the isotope envelope of the molecular ion was good in all cases. Some minor peaks resulted from fragmentation of the triethyleneglycol monomethyl ether groups at the dendrimer surface.

Demetallation to the highly air- and light-sensitive free-base porphyrins and iron insertion under conditions analogous to those employed for the preparation of the core [**4**·Fe^{III}]Cl finally yielded the target compounds [**1**·Fe^{III}]Cl, [**2**·Fe^{III}]Cl, and [**3**·Fe^{III}]Cl, which were purified by preparative GPC (*Bio-Rad Bio-Beads S-X3*; CH_2Cl_2) and shown by MALDI-TOF-MS to be free of structural defects (*Fig. 6*). The spectroscopic properties of the Fe^{III} porphyrin dendrimers were similar to those of the core [**4**·Fe^{III}]Cl. According to UV/VIS and EPR spectroscopy, they are six-coordinate low-spin complexes with double axial imidazole ligation. Reduction with $Na_2S_2O_4$ in

Scheme 2. *Synthesis of the Dendritic Cytochrome Mimics [**1**·Fe^{III}]Cl, [**2**·Fe^{III}]Cl, and [**3**·Fe^{III}]Cl and the Dendritic Wedge* **18**

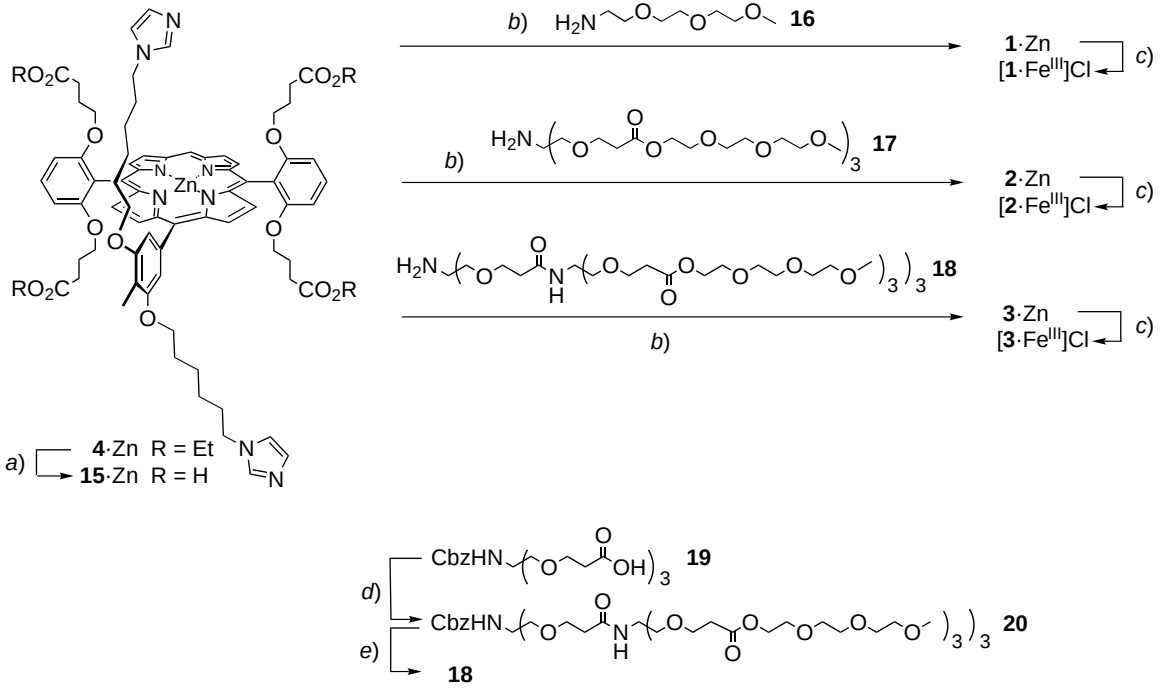

a) NaOH, dioxane/H_2O, r.t., 3 d. *b*) **16**, **17**, or **18**, HATU, Et_3N, DMF, 0°, 1 d; 85% (**1**·Zn); 3 d; 65% of **2**·Zn; 7 d, 42% of **3**·Zn); all yields starting from **4**·Zn. *c*) CF_3COOH, $CHCl_3$, 0°, 5 min; then $FeCl_2$, 2,6-lutidine , THF, reflux, 2–6 h; then air; then 1% HCl in $CHCl_3$, r.t., 5 min; then 'proton sponge', THF, r.t., 15 min; 68% of [**1**·Fe^{III}]Cl; 73% of [**2**·Fe^{III}]Cl; 78% of [**3**·Fe^{III}]Cl). *d*) **17**, BtOH, DCC, THF, r.t., 5 d; 58%. *e*) $HCOONH_4$, Pd/C (10%), EtOH, 40°, 6 h, 98%. HATU = *O*-(7-Azabenzotriazol-1-yl)-*N,N,N′,N′*-tetramethyluronium hexafluorophosphate; BtOH = 1-hydroxy-1*H*-benzotriazol; DCC = *N,N′*-dicyclohexylcarbodiimide; Cbz = benzyloxycarbonyl.

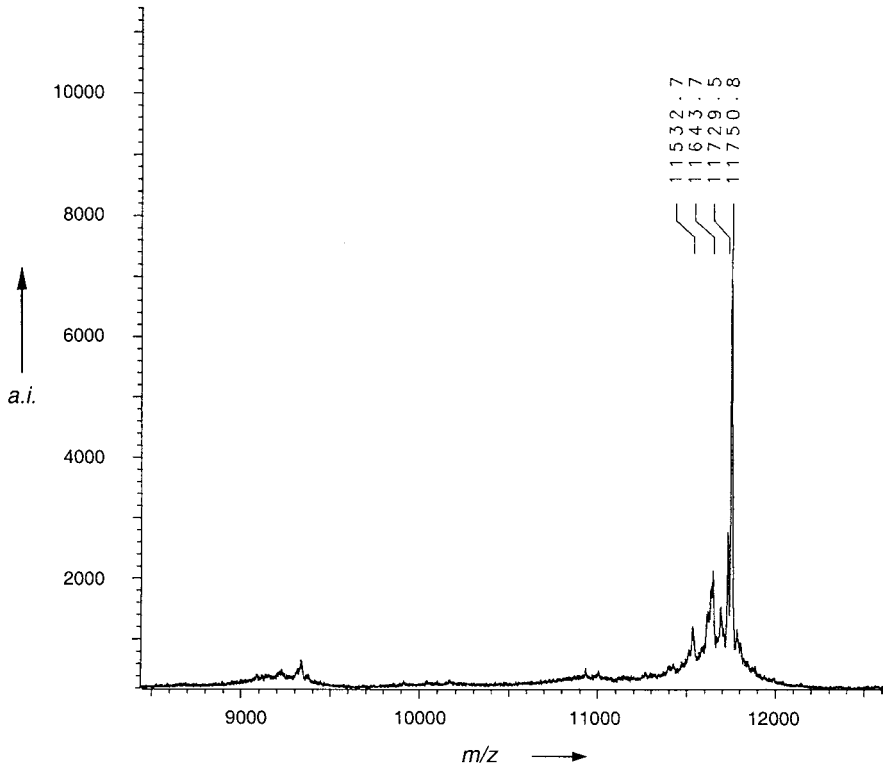

Fig. 5. *MALDI-TOF Mass spectrum of the dendritic Zn^{II} porphyrin* **3**·*Zn*. Matrix: 0.01M 2-(4-hydroxyphenylazo)benzoic acid (HABA) in MeCN/H_2O 4:1, analyte in CH_2Cl_2; reflector mode.

various solvents instantaneously gave electronic absorption spectra typical for low-spin Fe^{II} porphyrins, regardless of the size of the dendrimer, and re-oxidation to the Fe^{III} derivatives in air was similarly fast as well.

2.3. *Redox Properties of the Dendritic Iron Porphyrins.* The redox properties of [**1**·Fe^{III}]Cl, [**2**·Fe^{III}]Cl, and [**3**·Fe^{III}]Cl were first investigated in the rather nonpolar solvent CH_2Cl_2 by cyclic (CV) and steady-state voltammetry (SSV) (*Table*). All three compounds showed a reversible one-electron-reduction step (*Fig. 7*), which was clearly assigned to the Fe^{III}/Fe^{II} couple by spectroelectrochemical methods. The UV/VIS spectra of the electrochemically reduced species were identical to those obtained by chemical reduction, and well-defined isosbestic points evolved during controlled-potential electrolysis (*Fig. 8*). The generation-zero complex [**1**·Fe^{III}]Cl exhibited a redox potential of -0.21 V (*vs.* SCE; *Table*) for the Fe^{III}/Fe^{II} couple. This is in the expected range for a bis-imidazole-ligated iron-porphyrin complex [26]. In the higher-generation compounds [**2**·Fe^{III}]Cl ($+0.08$ V) and [**3**·Fe^{III}]Cl ($+0.10$ V), the $Fe^{III} \rightarrow Fe^{II}$ reduction becomes greatly facilitated (by 310 mV), with the largest change in potential (290 mV) occurring between generation zero and one.

CV Measurements in MeCN (*Fig. 7*), a solvent of intermediate polarity, showed a similar trend: upon changing from generation zero (-0.24 V) to two ($+0.09$ V),

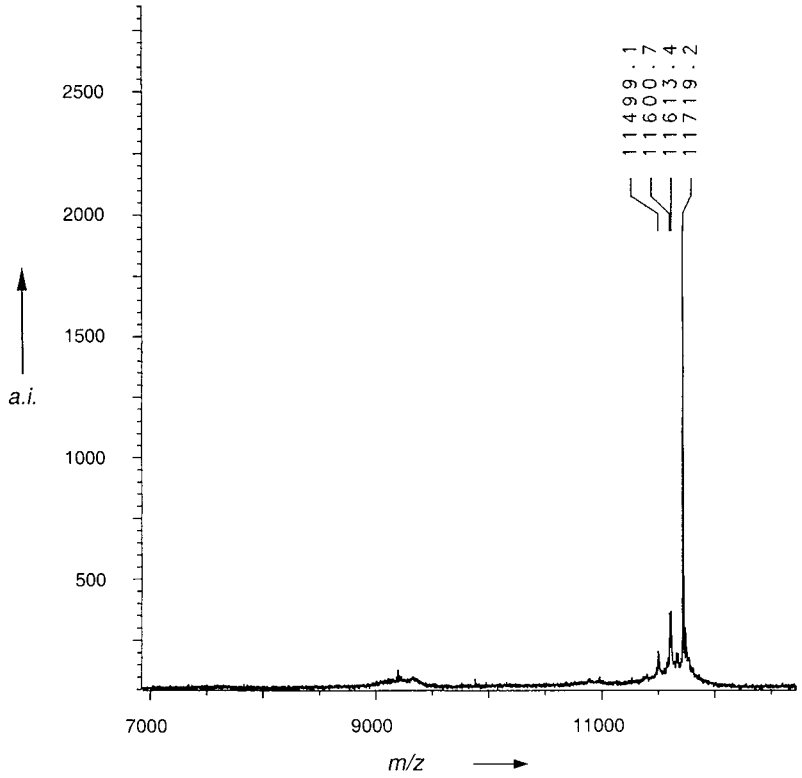

Fig. 6. *MALDI-TOF Mass spectrum of the dendritic Fe^{III} porphyrin [**3**·Fe^{III}]Cl.* Matrix: 0.01M HABA in MeCN/H_2O 4:1, analyte in CH_2Cl_2; reflector mode.

reduction of Fe^{III} becomes increasingly favored (by 330 mV) with the largest change in potential (by 230 mV) again occurring at the stage of the first generation dendrimer (−0.01 V).

In H_2O, the redox process could be monitored electrochemically for only the generation zero complex [**1**·Fe^{III}]Cl, with the generation-one dendrimer [**2**·Fe^{III}]Cl showing a very weak spread-out reduction step and the second-generation compound [**3**·Fe^{III}]Cl being electrochemically silent [10a]. Therefore, we changed to chemical methods to determine the redox potential for the Fe^{III}/Fe^{II} couple in this solvent. UV/VIS-Spectroscopic investigations showed that equilibria with solutions of suitable reducing agents were rapidly established after mixing with the oxidized Fe^{III} forms of the porphyrin dendrimers. This allowed an accurate, highly reproducible determination of the redox potentials from equilibrium measurements with $[Fe(ox)_3]^{-4/-3}$ [28a,b] (ox = oxalate) or $[Fe(CN)_6]^{-4/-3}$ [28c,d] (*Fig. 9*), as it has been commonly done with proteins (*Table*) [29].

The potentials measured for [**1**·Fe^{III}]Cl by chemical and electrochemical methods were in excellent agreement. In contrast to the results obtained in the organic solvents, the potential of the Fe^{III}/Fe^{II} couple hardly shifts upon changing from generation zero (−0.29 V) to one (−0.25 V), but a dramatic increase (by 340 mV) is observed upon

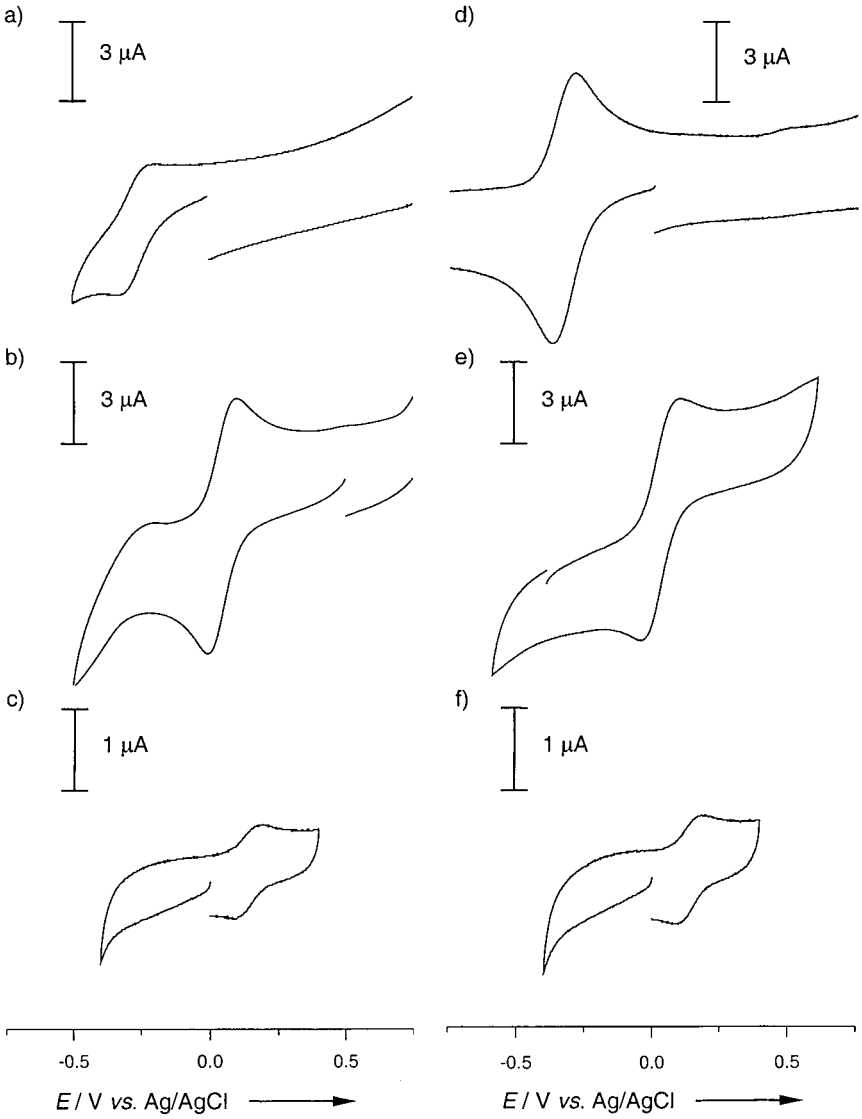

Fig. 7. *Cyclic voltammograms showing the first reduction step of [***1***· Fe^{III}]Cl (a, d), [***2***· Fe^{III}]Cl (b, e), and [***3***· Fe^{III}]Cl (c, f) in CH_2Cl_2* (left) *and MeCN* (right). Supporting electrolyte 0.1M Bu_4NPF_6; glassy-carbon working electrode; Ag/AgCl reference electrode; Pt wire counter electrode; $T = 298$ K; scan rate = 0.1 Vs^{-1}; typical concentration 0.5 mM; Fc was used as an internal standard.

changing to the generation two dendrimer [**3**·Fe^{III}]Cl (+0.09 V). For comparison, the Fe^{III}/Fe^{II} redox potential of cytochrome-b_5 in H_2O lies at −0.22 V *vs.* SCE [13b] and cytochrome-*c* in H_2O has a redox potential of −0.05 V *vs.* SCE [15b]. Over all three generations, the redox potential of the Fe^{III}/Fe^{II} couple in the generation two dendrimer

Table. *Redox Potentials* ([V], *vs.* SCE) *of the Fe^{III}/Fe^{II} Couple in [**1**·Fe^{III}]Cl, [**2**·Fe^{III}]Cl, and [**3**·Fe^{III}]Cl in Different Solvents*

Porphyrin	E (Fe^{III}/Fe^{II})		
	CH_2Cl_2 [a])	MeCN [a])	H_2O
[**1**·Fe^{III}]Cl	−0.21	−0.24	−0.29 [b])
[**2**·Fe^{III}]Cl	+0.08	−0.01	−0.25 [b])
[**3**·Fe^{III}]Cl	+0.10	+0.09	+0.09 [c])

[a]) Values from CV approximated as $E_{1/2}=(E_{pa}-E_{pc})/2$; supporting electrolyte 0.1M Bu_4NPF_6; glassy-carbon working electrode, Ag/AgCl reference electrode, Pt wire counter electrode; $T=298$ K; scan rate = 0.1 V s^{-1}; typical concentration $5\cdot10^{-4}$ M; Fc was used as an internal potential standard, and the redox potentials referenced against the standard calomel electrode (SCE) by means of published values for the Fc/Fc^+ couple in CH_2Cl_2 (0.46 V *vs.* SCE [27a]) and MeCN (0.45 V *vs.* SCE [27b]). [b]) Values from equilibrium measurements with $[Fe(ox)_3]^{-4/-3}$ as reference compound; $T=298$ K. E Values *vs.* the normal hydrogen electrode (NHE) were obtained from a nonlinear least-squares fit of the data from the series of equilibria produced by a titration to the *Nernst* equation and referenced for comparison against SCE (0.24 V *vs.* NHE [27c]). For detailed conditions, see *Exper. Part.* [c]) Values from equilibrium measurements with $[Fe(CN)_6]^{-4/-3}$ as reference compound; $T=$ 298 K. E Values were obtained as described above. For detailed conditions, see *Exper. Part.*

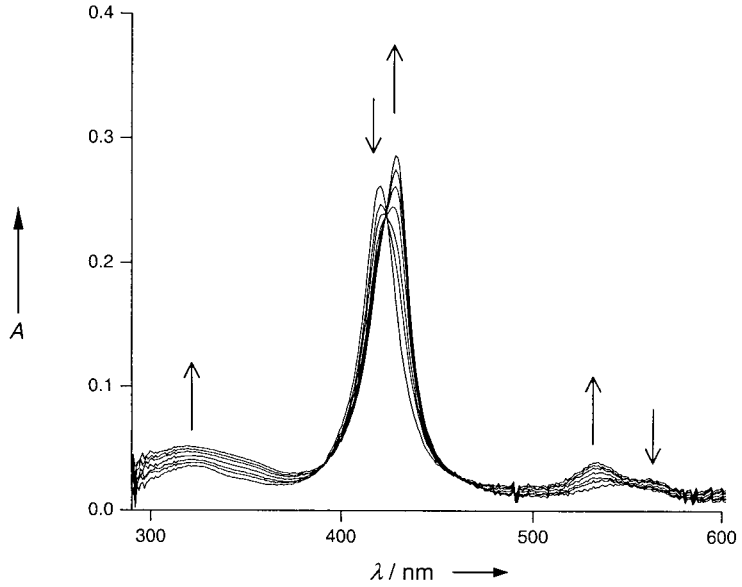

Fig. 8. *Time-Resolved UV/VIS spectroelectrochemistry on an optically transparent thin-layer electrode (OTTLE) in CH_2Cl_2 with 0.1M Bu_4NPF_6 upon controlled potential reduction of the dendritic Fe^{III} porphyrin [**1**·Fe^{III}]Cl, carried out at the first reduction step in the potential region of −0.21 V* vs. *SCE.* Well-defined isosbestic points are visible at 385, 418, and 438 nm.

increases by 380 mV. The results of the redox studies in the three solvents are summarized in *Fig. 10*.

3. Discussion and Conclusions. – This model study confirms the large contributions of the densely packed protein shell to the strong positive shifts of the Fe^{III}/Fe^{II} potential

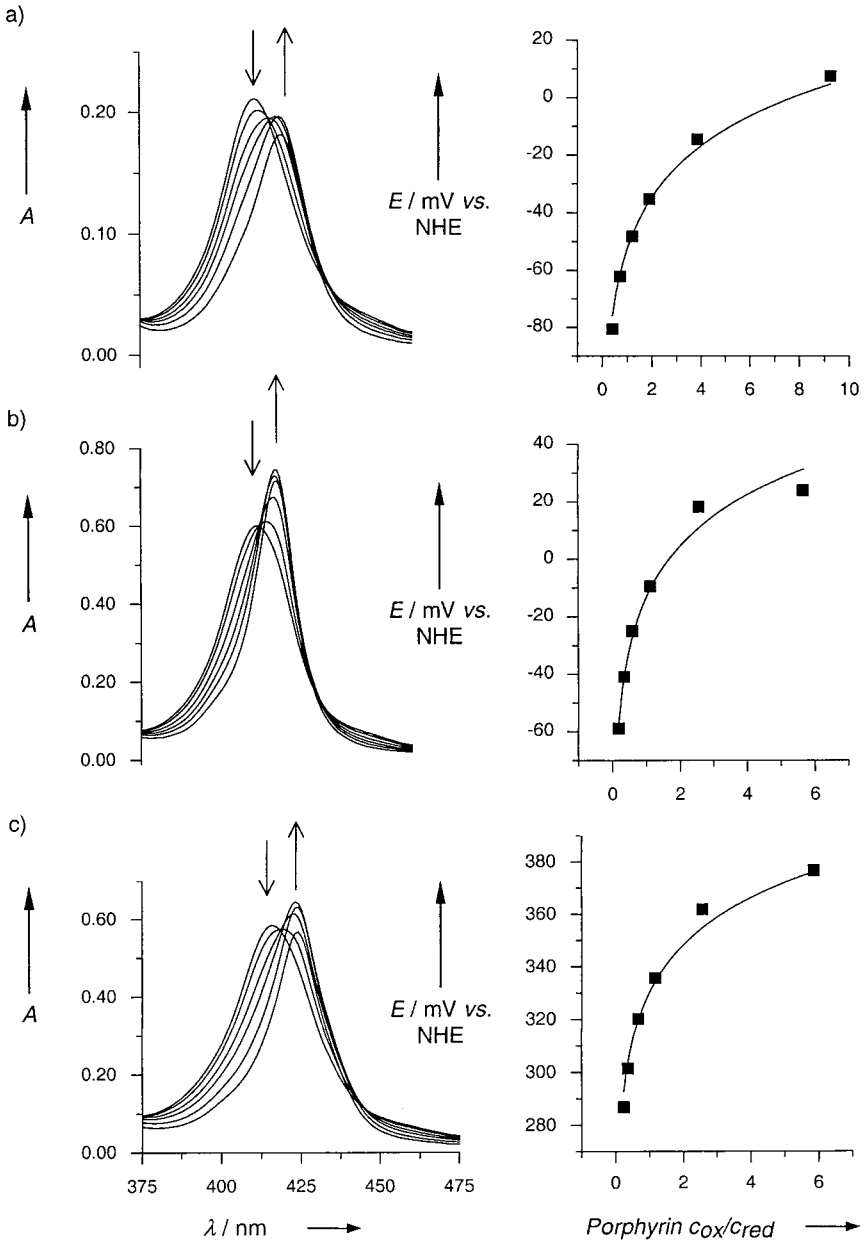

Fig. 9. *Redox equilibria in* H_2O *between* $[Fe(ox)_3]^{-4/-3}$ *and* [**1**·Fe^{III}]*Cl* (*a*), *and* [**2**·Fe^{III}]*Cl* (*b*) *and between* $[Fe(CN)_6]^{-4/-3}$ *and* [**3**·Fe^{III}]*Cl* (*c*). Spectral evolution of the *Soret*-band region in the UV/VIS spectrum during reductive titration (*left*) and nonlinear least-squares fit of the titration data to the *Nernst* equation, yielding the redox potential (*right*). A stock solution of fully oxidized porphyrin (typical concentration $5 \cdot 10^{-6}$ M) was titrated with a stock solution of fully reduced reference compound (typical concentration $2.5 \cdot 10^{-4}$ M), and the concentrations of all species in solution calculated at each titration point from the spectrophotometrically determined ratio of oxidized to reduced porphyrin and known total concentrations; $T = 298$ K.

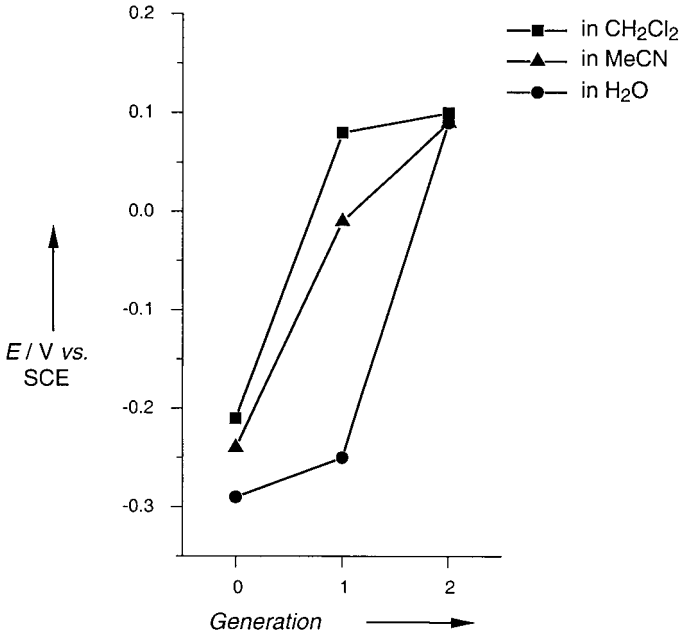

Fig. 10. *Plot of the redox potentials* ([V] *vs.* SCE) *of the* Fe^{III}/Fe^{II} *couple in* [**1**·Fe^{III}]Cl, [**2**·Fe^{III}]Cl, *and* [**3**·Fe^{III}]Cl *in* CH_2Cl_2, *MeCN, and* H_2O vs. *dendrimer generation*

in cytochromes [7a,b] and firmly establishes well-designed dendrimers as powerful mimics for globular proteins.

A number of important findings can be noted: *i*) in all solvents investigated, the redox potential of the Fe^{III}/Fe^{II} couple becomes more positive with increasing dendritic generation. Remarkably, the potential of the second-generation complex [**3**·Fe^{III}]Cl is, within experimental error, identical in all three solvents (of extremely different polarity), which clearly demonstrates that the dendritic branching creates a unique local microenvironment around the isolated electroactive core. Therefore, the dendritic shell fully mimics the protecting peptide shell, which modulates the redox potential of the Fe^{III}/Fe^{II} couple in a similar way in cytochromes [7a,b]. *ii*) In the two organic solvents, the largest shift to more positive potential occurs upon changing from the generation-zero to the generation-one complex. Clearly, the special microenvironment at the dendritic core is already largely created by the first generation branching in these solvents. *iii*) In sharp contrast, the redox potential in H_2O does not vary much upon passing from the generation-zero to the generation-one complex. Solvation effects are much more pronounced in H_2O, and, as we had previously suggested [9b,c], the relatively open dendritic branches in [**2**·Fe^{III}]Cl do not impede access of bulk solvent to the central core for stabilization of the Fe^{III} state. However, in [**3**·Fe^{III}]Cl, the dendritic superstructure is sufficiently dense to prevent the contact between heme and external bulk solvent, thereby creating the same, unique core microenvironment as in organic solvents. *iv*) The shift to more positive potentials with increasing dendritic generation in H_2O can be readily explained by the increased shielding of the electroactive core from

the polar bulk solvent. The reduced solvation of the charged Fe^{III} porphyrin core leads to an energetic destabilization of this state with respect to the charge-neutral Fe^{II} species, which is much less affected by the weaker solvation. In contrast, the analogous trend observed in the organic solvents is much harder to rationalize. As the two organic solvents employed are both considerably less polar than we estimate the dendritic shell with its secondary amide and triethyleneglycol monomethyl ether residues to be, one would rather expect a stabilization of the polar oxidized state with increasing encapsulation and exclusion of bulk solvent. Therefore, a lowering of the redox potential of the Fe^{III}/Fe^{II} couple with increasing dendritic generation would be expected to result. This is, however, clearly not the case. Obviously, there are other effects besides controlling solvent access and solvent-mediated charge stabilization, which the dendritic shell exerts upon the shielded electrophore at its core. These probably are related to its detailed chemical nature, conformation, and flexibility (which can vary largely in different solvents), as this strong influence of dendrimer generation on redox properties is not observed with some other types of dendrimers [10a]. There are certainly more studies required to achieve some understanding here, especially regarding the detailed structural and conformational properties of the dendrimers themselves. *v*) With increasingly tighter encapsulation of the electroactive core, the latter becomes less and less accessible for redox processes at the electrode surface, and, at higher generations, the electrochemical responses become occasionally too weak to be observable. This fact has been commonly observed in several studies with dendrimer-encapsulated electrophores and is well-accepted [9b,c][10a][11f,g] (for dendrimers with electroactive core functionality, see [30]). The finding that [**3** · Fe^{III}]Cl is not electrochemically silent in all solvents suggests that significantly different structures of the dendritic shell are present in the three solvents investigated here, and that the dendrimers probably display conformations with vastly different degrees of rigidity and average size ('hydrodynamic volume') [10d][31], depending on solvent composition. However, the absence of an electrochemical signal and the fact that bulk solvent seems to be excluded from the environment of the core does not diminish the possibility that small molecules (as well as individual solvent molecules) can, due to its flexible nature, easily penetrate the dendritic shell even at the highest generation studied here, and perform chemistry inside the dendrimer and even at the core. This was clearly shown by the feasibility of the $Fe^{III} \rightarrow Fe^{II}$ reduction with chemical reducing agents in the course of the equilibrium measurements described above.

This work was supported by the *ETH Research Council* and *F. Hoffmann-La Roche*, Basel.

Experimental Part

General. Reagents and solvents were purchased as reagent-grade and used without further purification unless otherwise stated. Compounds **7** · 2 H [9c], **9** [17], **16** [24], **17** [25], and **20** [25] were prepared according to published procedures or by slight modifications of such. Abs. THF and Et_2O was freshly distilled from sodium benzophenone ketyl, PhMe and PhH from Na metal, and CH_2Cl_2 and $CHCl_3$ from CaH_2. All reactions were performed in standard oven-dried glassware under N_2 except for reactions involving Fe^{II} compounds, which were carried out under Ar. Evaporation and concentration *in vacuo* was done at water-aspirator pressure, and compounds were dried under high vacuum (h.v.) at 10^{-3} Torr. Flash chromatography (FC): SiO_2–*H*, 5–40 μm, *Fluka*, with elution at 0.2–0.4 bar; SiO_2 *60*, 0.063–0.2 mm, *Fluka*, with elution at a maximum pressure of 0.1 bar; neutral alumina, *ICN Biomedicals* (type *B*, activity I), with elution at a maximum pressure of 0.1 bar.

TLC: *SiO_2 Alugram SIL G/UV_{254}*, *Macherey-Nagel* or *Alumina 60 type E/UV_{254}*, *Merck*, visualization by UV light at 254 nm and 366 nm, or by heating after coloring with 'Mostain' soln. (10% aq. H_2SO_4 soln. (400 ml), $(NH_4)_6Mo_7O_{24}\cdot 6\,H_2O$ (20 g), and $Ce(SO_4)_2$ (0.6 g)). Prep. gel permeation chromatography (GPC): open glass columns (5×200 cm or 10×200 cm) with *Bio-Rad Bio-Beads S-X1*, *Bio-Rad Bio-Beads S-X3*, or *Pharmacia Sephadex LH-20*, or for high-performance gel-permeation chromatography (HP-GPC) a *Merck-Hitachi* prep. HPLC system with pump *L-7100* and UV detector *L-7400* and a prep. *NovoGROM* 100 column (2.5×30 cm) and THF at a flow-rate of 0.50 ml/min as the eluent. Anal. GPC: *Merck-Hitachi* HPLC system with pump *L-7100*, column oven *L-7360*, and UV detector *L-7400*, and a serial two-column setup with one *Shodex GPC KF-802.5* and one *Shodex GPC KF-803L* anal. GPC column, and with THF at a flow rate of 1.00 ml/min as the eluent. M.p.: *Büchi B-510* or *Büchi B-540* apparatus; uncorrected. UV/VIS Spectra (λ_{max} in nm (ε [l mol^{-1} cm^{-1}])): *Varian Cary 5* spectrometer. IR Spectra [cm^{-1}]: *Perkin-Elmer 1600-FTIR*. NMR Spectra (δ in ppm (*J* in Hz)): *Bruker AM-500* and *Varian Gemini 300* or *200* at 297 K, with solvent peaks as reference. EPR Spectra: *Varian E12 EPR* with *Bruker ER-035M NMR Gaussmeter* at 9.24419 GHz with a microwave power of 100 mW; diphenylpicrylhydrazyl (DPPH) was used as reference. MALDI-TOF-MS: *Bruker REFLEX* spectrometer; matrices used are indicated with the spectra and consisted either of 2-(4-hydroxyphenylazo)benzoic acid (HABA), or 2,4,6-trihydroxyacetophenone (THA) and ammonium citrate; positive-ion mode at 20 kV acceleration voltage, reflector mode. FAB-MS: *VG ZAB 2SEQ* Instrument; 3-nitrobenzyl alcohol (NOBA) as matrix. ESI-MS: *7T-Finnigan Newstar FT/MS System*, MeOH as solvent and poly(methyl methacrylate) as internal reference. Magnetic moments $\mu_{eff}^{25°}$ (μ_B) were determined by the *Evans-Scheffold* method in deuterated solvents with 2% Me_4Si or *t*-BuOH as reference compounds [22]. Elemental analyses were performed by the Mikrolabor at the Laboratorium für Organische Chemie, ETH-Zürich.

General Procedure 1 (*GP 1*): *Hydrolysis of Porphyrin Tetraethyl Ester to Porphyrin Tetra-acid.* The porphyrin tetraethyl ester (0.020 mmol) was dissolved in dioxane (2 ml), and 2M NaOH (2 ml) was added. The two-phase system was vigorously stirred in the dark at r.t. for 3 d. The mixture was extracted with $CHCl_3$ (10 ml), and the deep purple aq. phase was carefully acidified with 0.5M HCl, until a stable, voluminous purple precipitate formed. The resulting suspension was saturated with NaCl by addition of solid NaCl, upon which the voluminous precipitate aggregated to form black crystals, which were filtered off. The crude porphyrin tetra-acid was washed with H_2O (10 ml), acetone (5 ml), and Et_2O (25 ml), and dried under h.v. in the dark for 2 h.

General Procedure 2 (*GP 2*): *Zn^{II} to Fe^{II} Metal Exchange in the Dendritic Porphyrins.* A deep purple soln. of the dendritic Zn^{II} porphyrin (0.010 mmol) in abs. $CHCl_3$ (10 ml) was carefully degassed by 3 'freeze-pump-thaw' cycles and then cooled to 0° in an ice bath. Subsequently, CF_3COOH (23.0 µl, 0.300 mmol) was added, and the dark-green soln. was stirred at r.t. for 5 min. The resulting mixture was titrated with 2,6-lutidine until its color changed to brown-purple and then washed with degassed H_2O (3×10 ml). The aq. phase was removed between washings and, at the end, with a syringe equipped with a long, thin needle. All solvent was then distilled off under h.v. at r.t., and the residue of free-base porphyrin was dried under h.v. for 2 h. The crude, amorphous product was dissolved in abs. THF (15 ml), 2,6-lutidine (8.7 µl, 0.075 mmol) was added, and the soln. was heated to reflux for 15 min. The brown-purple soln. was then treated with anh. $FeCl_2$ (19.0 mg, 0.150 mmol) and heated to reflux for 2–6 h. After cooling of the now red-brown soln. to r.t., the mixture was exposed to air with stirring for 30 min, to ensure complete oxidation to the Fe^{III} complex. Subsequently, the mixture was filtered through a 1-cm layer of *Celite*, then concentrated *in vacuo*, and dried under h.v. The residue was dissolved in $CHCl_3$ (5 ml), 1% HCl in $CHCl_3$ (20 ml) was added, and the mixture was stirred at r.t for 5 min. The solvent was evaporated *in vacuo*, and the dark brown residue was taken up in abs. THF (10 ml). The resulting soln. was treated with 1,8-bis(dimethylamino)naphthalene (34.3 mg, 0.160 mmol), upon which its color changed from dark-brown to red-brown. The mixture was stirred at r.t. for an additional 15 min, concentrated *in vacuo*, and the crude, oily product was subjected to prep. GPC (*Bio-Beads S-X3*; CH_2Cl_2). The pure dendritic Fe^{III} porphyrin was finally dried under h.v. for at least 3 d.

General Procedure 3 (*GP 3*): *Reduction of Dendritic Fe^{III} Porphyrins to the Corresponding Fe^{II} Complexes.* The reductions were carried out under homogenous conditions in aq. soln. A *ca.* $5\cdot 10^{-6}$ M soln. of dendritic Fe^{III} porphyrin in H_2O (2.00 ml) was degassed by bubbling Ar through for 30 min and subsequently transferred into a septum-sealed, Ar-flushed quartz cuvette (optical path length 1.000 cm) *via* canula. A freshly prepared 0.1M soln. of $Na_2S_2O_4$ in degassed H_2O (10 µl) was added, the mixture was shaken for 30–90 s, and the reduced dendritic Fe^{II} porphyrin was then analyzed by UV/VIS spectroscopy. The color of the porphyrin soln. changed from red-brown to bright-orange upon reduction.

*Tetraethyl 4,4′,4″,4‴-[10-Bromo-21*H*,23*H*-porphine-5,15-diylbis(benzene-2,1,3-triyldioxy)]tetrakis(butanoate)* (**5**·2 H). To **8**·2 H (399 mg, 0.35 mmol) in abs. PhH (15 ml) under reflux, Bu_3SnH (0.139 ml, 0.53 mmol) was added, immediately followed by AIBN (5 mg (cat.)), and the mixture was heated to reflux for

2 h. After cooling to r.t., the solvent was evaporated, and the black, oily residue was dissolved in MeCN (50 ml) and extracted with hexane (5 × 25 ml). The MeCN layer was concentrated *in vacuo*, and the residue was dried under h.v. The remaining dark oil was purified by FC (SiO_2–*H* (250 g); $CHCl_3$/AcOEt 98:2). Product-containing fractions were concentrated to *ca.* 1 ml, and hexane (10 ml) was added. The resulting crystalline precipitate was filtered off and dried under h.v. to yield **5**·2 H (159 mg, 43%). Brown-purple powder. M.p. 115°. TLC (SiO_2; $CHCl_3$/AcOEt 98:2): R_f 0.41. UV/VIS ($CHCl_3$): 588 (4300), 545 (3800), 511 (15600), 416 (306800). IR (KBr): 3677*w*, 3611*w*, 3022*m*, 2966*w*, 1727*s*, 1588*w*, 1450*m*, 1244*m*, 1188*m*, 1100*s*, 1038*w*, 666*s*. ^{1}H-NMR (200 MHz, $CDCl_3$): 10.07 (*s*, 1 H); 9.66 (*d*, *J* = 4.8, 2 H); 9.22 (*d*, *J* = 4.8, 2 H); 8.90 (*d*, *J* = 4.8, 2 H); 8.88 (*d*, *J* = 4.8, 2 H); 7.73 (*t*, *J* = 8.4, 2 H); 7.04 (*d*, *J* = 8.4, 4 H); 3.93 (*t*, *J* = 4.9, 8 H); 3.65 (*q*, *J* = 7.1, 8 H); 1.20–1.30 (*m*, 16 H); 0.83 (*t*, *J* = 7.1, 12 H); −2.85 (*s*, 2 H). ^{13}C-NMR (50 MHz, $CDCl_3$): 172.2; 159.7; 149.1–150.2 (4 br.); 132.1; 131.1; 130.4 (2×); 119.7; 112.5; 105.4; 104.5; 67.3; 59.7; 29.5; 23.7; 13.7; 2 signals not observed due to signal overlap. FAB-MS: 1062.3 (100, M^+). Anal. calc. for $C_{56}H_{61}BrN_4O_{12}$ (1062.02): C 63.33, H 5.79, N 5.28; found: C 63.39, H 5.96, N 5.28.

*(*SP*-4-2)-[[Tetraethyl 4,4′,4″,4‴-[10-Bromo-21*H*,23*H*-porphine-5,15-diylbis(benzene-2,1,3-triyldioxy)]tetrakis-(butanoato)](2−)-*N^{21},N^{22},N^{23},N^{24}*]zinc(II)* (**5**·Zn). A mixture of **5**·2 H (139 mg, 0.12 mmol) and $Zn(OAc)_2$·2 H_2O (266 mg, 1.20 mmol) in $CHCl_3$/MeOH 1:1 (10 ml) was heated to reflux for 60 min. The resulting deep-purple soln. was evaporated to dryness *in vacuo*. The residue was taken up in CH_2Cl_2 (30 ml) and extracted with H_2O (3 × 15 ml). The soln. was concentrated *in vacuo* and the residue dried under h.v. The crude product was recrystallized from THF/cyclohexane to yield **5**·Zn (106 mg, 78%). Purple needles. M.p. 139–141°. TLC (SiO_2; $CHCl_3$/AcOEt 98:2): R_f 0.32. UV/VIS ($CHCl_3$): 605 (4800), 555 (15000), 423 (364500), 403 (sh, 41000). IR (KBr): 2996*w*, 1725*s*, 1587*m*, 1456*s*, 1246*m*, 1180*w*, 1102*s*, 994*m*. ^{1}H-NMR (200 MHz, $CDCl_3$): 10.26 (*s*, 1 H); 9.89 (*d*, *J* = 4.7, 2 H); 9.44 (*d*, *J* = 4.7, 2 H); 9.14 (*d*, *J* = 4.7, 2 H); 9.12 (*d*, *J* = 4.7, 2 H); 7.92 (*t*, *J* = 8.3, 2 H); 7.23 (*d*, *J* = 8.3, 4 H); 4.08 (*t*, *J* = 5.8, 8 H); 3.50 (*q*, *J* = 7.1, 8 H); 1.15–1.50 (*m*, 16 H); 0.85 (*t*, *J* = 7.1, 12 H). ^{13}C-NMR (50 MHz, $CDCl_3$): 172.7; 159.7; 150.8; 150.8; 150.0; 148.9; 132.5; 132.0; 131.8; 130.1; 121.9; 112.9; 106.4; 105.4; 103.7; 101.9; 67.8; 59.7; 29.3; 23.8; 13.6. FAB-MS: 1124.3 (100, M^+). Anal. calc. for $C_{56}H_{59}BrN_4O_{12}$ (1125.40): C 59.77, H 5.28, N 4.98; found: C 59.78, H 5.26, N 4.93.

*Tetraethyl 4,4′,4″,4‴-[10,20-Dibromo-21*H*,23*H*-porphine-5,15-diylbis(benzene-2,1,3-triyldioxy)]tetrakis-(butanoate)* (**8**·2 H). A soln. of **7**·2 H (984 mg, 1.00 mmol) [9c] in $CHCl_3$ (100 ml) was cooled to 0° in an ice bath. NBS (356 mg, 2.00 mmol) in $CHCl_3$ (350 ml) was added dropwise, and the mixture was stirred at 0° for 30 min. After addition of acetone (50 ml), the solvent was evaporated *in vacuo*. The resulting black residue was purified by FC (SiO_2–*H* (350 g); $CHCl_3$/AcOEt 97:3). Fractions containing the product were reduced to a total volume of *ca.* 5 ml *in vacuo*. Hexane (50 ml) was added, and the resulting crystalline precipitate was filtered off and dried under h.v. to give **8**·2 H (1.038 g, 91%). Brown-purple powder. M.p. 136°. TLC (SiO_2; $CHCl_3$/AcOEt 98:2): R_f 0.55. UV/VIS ($CHCl_3$): 601 (4000), 554 (7500), 520 (15000), 423 (309500). IR (KBr): 3432*w*, 2934*w*, 1727*s*, 1582*m*, 1459*m*, 1246*w*, 1181*w*, 1096*m*, 963*w*, 794*w*, 717*w*. ^{1}H-NMR (200 MHz, $CDCl_3$): 9.55 (*d*, *J* = 5.0, 4 H); 8.80 (*d*, *J* = 5.0, 4 H); 7.73 (*t*, *J* = 8.3, 2 H); 7.03 (*d*, *J* = 8.3, 4 H); 3.94 (*t*, *J* = 4.6, 8 H); 3.67 (*q*, *J* = 7.0, 8 H); 1.24–1.44 (*m*, 16 H); 0.85 (*t*, *J* = 7.0, 12 H); −2.48 (*s*, 2 H). ^{13}C-NMR (50 MHz, $CDCl_3$): 172.2; 158.9; 148.2–149.3 (2 br.); 130.1–131.6 (2 br.); 129.9; 119.1; 112.6; 104.6; 101.9; 66.6; 59.1; 28.8; 23.0; 13.1. FAB-MS: 1140.2 (100, M^+). Anal. calc. for $C_{56}H_{60}Br_2N_4O_{12}$ (1140.92): C 58.95, H 5.30, N 4.91; found: C 58.83, H 5.52, N 4.95.

5-Bromo-2-methylbenzene-1,3-diol (**10**). *5-Bromo-1,3-dimethoxy-2-methylbenzene* (**9**; 4.62 g, 20.0 mmol) [17] in AcOH (50 ml) was mixed with stabilized 56% aq. HI soln. (40 ml), upon which a white, voluminous precipitate formed. The mixture was heated to reflux and became a clear soln. After heating the soln. for 6 h and cooling to r.t., 5% aq. $NaHSO_3$ soln. (300 ml) was added, and the resulting yellow suspension was extracted with Et_2O (5 × 75 ml). The combined org. phases were washed with H_2O (100 ml), dried ($MgSO_4$), and evaporated to dryness. The obtained yellow solid was dried under h.v. overnight and subsequently dissolved in boiling $CHCl_3$ (50 ml). After slow addition of hexane (150 ml) and cooling to r.t., crystallization was completed by standing at 4° for 2 h. Filtration and drying under h.v. yielded **10** (3.80 g, 94%). Colorless needles. M.p. 124°. TLC (SiO_2; hexane/AcOEt 75:25): R_f 0.42. IR (KBr): 3411*s* (br.), 3335*s*, 1610*s*, 1508*m*, 1446*m*, 1404*s*, 1342*m*, 1275*s*, 1056*vs*, 866*s*, 813*s*, 707*w*, 565*w*. ^{1}H-NMR (200 MHz, $(CD_3)_2SO$): 9.55 (br. *s*, 2 H); 6.46 (*s*, 2 H); 1.88 (*s*, 3 H). ^{13}C-NMR (50 MHz, $(CD_3)_2SO$): 157.3; 117.5; 109.7; 108.9; 8.3. EI-MS: 204 (95, M^+, $C_7H_7{}^{81}BrO_2$), 202 (100, M^+, $C_7H_7{}^{79}BrO_2$), 123 (42, $[M-Br]^+$). Anal. calc. for $C_7H_7BrO_2$ (203.04): C 41.41, H 3.47, Br 39.35; found: C 41.44, H 3.61, Br 39.14.

5-Bromo-1,3-bis(methoxymethoxy)-2-methylbenzene (**11**). To **10** (0.812 g, 4.0 mmol) in MeCN (40 ml) cooled to 0° in an ice bath, anh. K_2CO_3 (4.423 g, 32.0 mmol) was added, and the suspension was stirred for 30 min. MOM-Cl (122 ml, 16.0 mmol) was added dropwise, and the mixture was left to warm to r.t. overnight. MeOH (20 ml) was added, and the mixture was stirred at r.t. for 8 h. The solvent was evaporated *in vacuo*, H_2O

(50 ml) was added to the residue, and the resulting mixture was extracted with AcOEt (3 × 25 ml). The combined org. phases were washed with 1M NaOH (25 ml), dried ($MgSO_4$), and concentrated *in vacuo*. The resulting yellow oil was purified by FC (SiO_2 (15 g); hexane/AcOEt/Et_3N 95 : 4 : 1) and dried under h.v., upon which it slowly solidified to yield **11** (1.118 g, 96%). Colorless, waxy solid. M.p. 38°. TLC (SiO_2; hexane/AcOEt/Et_3N 95 : 4 : 1): R_f 0.51. IR (KBr): 2957*m*, 1589*s*, 1479*m*, 1427*m*, 1384*m*, 1312*w*, 1270*w*, 1235*w*, 1156*s*, 1121*s*, 1062*s*, 921*m*, 887*w*, 845*m*, 817*m*, 742*w*, 672*w*, 568*w*. ^{1}H-NMR (200 MHz, $CDCl_3$): 6.95 (*s*, 2 H); 5.17 (*s*, 4 H); 3.48 (*s*, 6 H); 2.09 (*s*, 3 H). ^{13}C-NMR (50 MHz, $CDCl_3$): 156.6; 119.1; 115.9; 111.7; 94.8; 56.1; 8.4. EI-MS: 292 (14, M^+, $C_{11}H_{15}{}^{81}BrO_4$), 290 (14, M^+, $C_{11}H_{15}{}^{79}BrO_4$), 45 (100, $[CH_2OCH_3]^+$). Anal. calc. for $C_{11}H_{15}BrO_4$ (291.14): C 45.38, H 5.19, Br 27.45; found: C 45.43, H 5.24, Br 27.52.

2-[3,5-Bis(methoxymethoxy)-4-methylphenyl]-4,4,5,5-tetramethyl-1,3,2-dioxaborolane (**12**). A soln. of TMEDA (0.96 ml, 6.40 mmol) in abs. THF (8 ml) was cooled to −78° and treated with 1.6M BuLi in hexane (4.00 ml, 6.40 mmol). After stirring for 30 min at −78°, a soln. of **11** (1.164 g, 4.00 mmol) in abs. THF (12 ml) was added dropwise during 10 min. The mixture was stirred for 1 h at −78°, upon which a white suspension formed. $B(OMe)_3$ (2.28 ml, 20.00 mmol) was added rapidly *via* syringe, and the mixture was stirred for another 2 h at −78° and then slowly warmed to r.t. After 1 h at r.t., sat. aq. NH_4Cl soln. (5.0 ml) was added. The resulting white suspension was extracted with CH_2Cl_2 (3 × 10 ml), and the combined org. layers were dried ($MgSO_4$) and evaporated *in vacuo*. The resulting colorless, thick oil was taken up in PhH (10 ml), and pinacol (4.720 g, 40.00 mmol) was added. After heating under reflux overnight with continuous azeotropic removal of H_2O with a *Dean-Stark* trap and cooling to r.t., the mixture was washed with H_2O (5 × 20 ml), and the org. phase was concentrated *in vacuo*. Drying of the residue under h.v. provided **12** (1.312 g, 97%). Colorless, crystalline solid. M.p. 113–114°. TLC (SiO_2; hexane/AcOEt/Et_3N 95 : 4 : 1): R_f 0.21. IR (KBr): 2976*m*, 1576*m*, 1422*s*, 1392*s*, 1356*s*, 1160*s*, 1116*s*, 1058*vs*, 993*m*, 966*m*, 919*m*, 851*m*, 711*w*, 694*m*, 675*w*. ^{1}H-NMR (200 MHz, $CDCl_3$): 7.15 (*s*, 2 H); 5.25 (*s*, 4 H); 3.51 (*s*, 6 H); 2.20 (*s*, 3 H); 1.33 (*s*, 12 H). ^{13}C-NMR (50 MHz, $CDCl_3$): 155.7; 128.4; 120.8; 113.8; 94.7; 83.8; 56.2; 24.8; 8.9. EI-MS: 338 (36, M^+), 45 (100, $[CH_2OCH_3]^+$). Anal. calc. for $C_{17}H_{27}BO_6$ (338.21): C 60.37, H 8.05; found: C 60.19, H 8.15.

2-Methyl-5-(4,4,5,5-tetramethyl-1,3,2-dioxaborolan-2-yl)benzene-1,3-diol (**13**). Conc. aq. HCl soln. (1.00 ml) was added to **12** (1.049 g, 3.10 mmol) in THF (50 ml) and MeOH (25 ml). The mixture was stirred at r.t. for 3 d and subsequently poured onto ice-water (100 ml). The resulting yellow soln. was extracted with CH_2Cl_2 (3 × 50 ml), and the combined org. layers were washed with H_2O (50 ml) and dried ($MgSO_4$). The soln. was concentrated *in vacuo* to *ca*. 50 ml, $CHCl_3$ (50 ml) was added, and all solvent was evaporated *in vacuo*. The remaining yellow solid was taken up as a slurry in 10 ml of $CHCl_3$ (10 ml), and, after exposure to an ultrasonic bath for 5 min, the solid crystalline material was filtered off. Washing with $CHCl_3$ and drying under h.v. afforded **13** (0.383 g, 51%). Colorless, crystalline powder. M.p. 202–204°. TLC (SiO_2; CH_2Cl_2/MeOH 95 : 5): R_f 0.59. IR (KBr): 3378*s* (br.), 2978*m*, 1578*m*, 1523*w*, 1420*s*, 1388*s*, 1299*s*, 1171*m*, 1140*s*, 1089*s*, 967*m*, 928*w*, 850*m*, 824*w*, 756*m*, 692*w*. ^{1}H-NMR (200 MHz, $(CD_3)_2SO$): 9.03 (*s*, 2 H); 6.65 (*s*, 2 H); 1.95 (*s*, 3 H); 1.26 (*s*, 12 H). ^{13}C-NMR (50 MHz, $(CD_3)_2SO$): 155.6; 113.7; 111.7; 111.5; 83.0; 23.4; 8.4. EI-MS: 250 (63, M^+), 164 (47), 150 (100). Anal. calc. for $C_{13}H_{19}BO_4 \cdot H_2O$ (268.10): C 58.24, H 7.89; found.: C 58.02, H 7.51.

*1-(6-Bromohexyl)-1*H*-imidazole Hydroacetate* (**14** · AcOH) [18]. To a suspension of NaH (1.20 g, 60.0 mmol) in abs. THF (40 ml), a soln. of imidazole (3.88 g, 60.0 mmol) in abs. THF (160 ml) was added within 5 min, and the resulting mixture was stirred at r.t. for 60 min. 1,6-Dibromohexane (29.20 ml, 180.0 mmol) was added in one portion, and the white suspension was stirred overnight at r.t. The precipitate formed was isolated by filtration and washed with Et_2O (2 × 40 ml). The combined filtrate and washings were evaporated at r.t. *in vacuo*, and the oily residue was redissolved in Et_2O (300 ml). The soln. was washed with H_2O (3 × 50 ml), and the org. phase was dried (Na_2SO_4) and reduced *in vacuo* to a volume of *ca*. 100 ml. This colorless soln. was purified by FC (SiO_2 (200 g); Et_2O/THF 50 : 50). The product-containing fraction was immediately cooled to 0° in an ice bath, and AcOH (6.86 ml, 120.0 mmol) was added. The solvent was removed *in vacuo*, and the oily residue was dried under h.v. to give **14** · AcOH (9.68 g, 55%). The product contains 1 additional equiv. of AcOH according to ^{1}H-NMR. Colorless viscous oil. B.p. 141–143° (dec.). TLC (SiO_2; Et_2O/THF 33 : 66): R_f 0.61. IR (Film): 3411*m* (br.), 3133*m*, 2933*s*, 2856*m*, 1711*s*, 1556*m*, 1516*m*, 1400*m*, 1367*m*, 1261*s*, 1083*m*, 1033*w*, 1011*w*, 840*w*, 744*w*. ^{1}H-NMR (200 MHz, $CDCl_3$): 7.94 (br. *s*, 2 H); 7.68 (*s*, 1 H); 7.10 (*s*, 1 H); 7.68 (*s*, 1 H); 3.96 (*t*, J = 7.1, 2 H); 3.40 (*t*, J = 6.6, 2 H); 2.09 (*s*, 6 H); 1.73–1.94 (*m*, 4 H); 1.23–1.57 (*m*, 4 H). ^{13}C-NMR (75 MHz, $CDCl_3$): 175.9; 136.4; 126.4; 119.0; 47.5; 33.4, 32.2; 30.5; 27.4; 25.5; 21.3. EI-MS: 232 (9, $[M - AcOH]^+$, $C_9H_{15}{}^{81}BrN_2$), 230 (9, $[M - AcOH]^+$, $C_9H_{15}{}^{79}BrN_2$), 205 (13, $[M - AcOH - HCN]^+$, $C_8H_{14}{}^{81}BrN$), 203 (14, $[M - AcOH - HCN]^+$, $C_8H_{14}{}^{79}BrN$), 151 (100, $[M - AcOH - Br]^+$).

*2-{3,5-Bis[6-(1*H*-imidazol-1-yl)hexyloxy]-4-methylphenyl}-4,4,5,5-tetramethyl-1,3,2-dioxaborolane* (**6**). Compound **14** · AcOH (365 mg,1.25 mmol) was dissolved in CH_2Cl_2 (20 ml), and the soln. was rapidly extracted

with 1M KOH (10 ml) at 0°. After drying the org. layer thoroughly (Na_2SO_4), abs. DMF (3 ml) was added, and the soln. was concentrated *in vacuo* at r.t. The resulting colorless soln. was added to **13** (63 mg, 0.25 mmol) in abs. DMF (5 ml), then anh. Cs_2CO_3 (482 mg, 1.50 mmol) was added, and the mixture was stirred at r.t. for 16 h. The resulting suspension was diluted with CH_2Cl_2 (30 ml), filtered through a 1-cm layer of *Celite*, and CH_2Cl_2 was evaporated *in vacuo* at r.t. The remaining DMF was distilled off under h.v. at 40°. Rapid FC with a short column of large diameter (SiO_2 (15 g); CH_2Cl_2/MeOH 95:5) and drying under h.v. provided **6** (67 mg, 49%) as a colorless, highly viscous oil that crystallized very slowly at −20°. Colorless, waxy solid. M.p. 63–66°. TLC (SiO_2; CH_2Cl_2/MeOH 95:5): R_f 0.11. IR ($CHCl_3$): 2963*m*, 2932*m*, 1570*w*, 1509*m*, 1476*w*, 1409*m*, 1356*m*, 1232*s*, 1203*s*, 1133*m*, 1073*w*, 1046*m*, 963*w*, 927*m*, 877*w*, 851*m*, 801*s*, 732*s*, 712*s*, 665*s*, 626*w*. ^{1}H-NMR (400 MHz, $CDCl_3$): 7.46 (*s*, 2 H); 7.05 (*s*, 2 H); 6.92 (*s*, 2 H); 6.90 (*s*, 2 H); 4.00 (*t*, *J* = 6.2, 4 H); 3.94 (*t*, *J* = 7.1, 4 H); 2.11 (*s*, 3 H); 1.74–1.85 (*m*, 8 H); 1.48–1.56 (*m*, 4 H); 1.33–1.41 (*m*, 4 H); 1.33 (*s*, 12 H). ^{13}C-NMR (100 MHz, $CDCl_3$): 157.4; 137.1; 129.4; 118.8; 118.7; 110.3; 104.5; 83.7; 68.1; 47.0; 31.1; 29.0; 26.1; 25.6; 24.9; 8.7. FAB-MS: 551.2 (100, MH^+). HR-FAB$^+$-MS: 551.3764 (M^+, $C_{31}H_{47}N_4O_4^+$; calc. 551.3768).

*(*SP*-4-2)-[{Tetraethyl 4,4′,4″,4‴-[10-(3,5-Bis{[6-(1*H*-imidazole-1-yl)hexyl]oxy}-4-methylphenyl)-21*H*,23*H*-porphine-5,15-diylbis(benzene-2,1,3-triyldioxy)]tetrakis(butanoato)}(2−)-*N^{21},N^{22},N^{23},N^{24}*]zinc(II)* (**4**·Zn). A suspension of **5**·Zn (112.5 mg, 0.100 mmol), **6** (137.6 mg, 0.250 mmol), anh. Cs_2CO_3 (154.0 mg, 0.800 mmol), and $[Pd(PPh_3)_4]$ (16.1 mg, 0.010 mmol) in abs. PhMe (20 ml) and abs. THF (10 ml) was carefully degassed by 5 'freeze-pump-thaw' cycles. The mixture was placed in a preheated oil bath and heated to reflux for 6 h in the dark. After cooling to r.t., CH_2Cl_2 (50 ml) was added, and the suspension was filtered through a 1-cm layer of *Celite*. The soln. was concentrated *in vacuo*, and the crude product was purified by FC (SiO_2–*H* (25 g); CH_2Cl_2/MeOH 99:1 → 95:5). The resulting purple solid was dried under h.v. and recrystallized from $CHCl_3$/heptane at −20°. Drying under h.v. yielded **4**·Zn (120.2 mg, 82%). Fine purple needles. M.p. 96°. TLC (SiO_2; CH_2Cl_2/MeOH 95:5): R_f 0.33. UV/VIS ($CHCl_3$): 597 (6200), 560 (20000), 427 (527800), 405 (42800), 312 (21900). IR (KBr): 2933*m*, 2856*w*, 1722*s*, 1578*m*, 1517*w*, 1456*s*, 1406*w*, 1378*w*, 1239*m*, 1177*m*, 1122*m*, 1094*s*, 1056*w*, 1028*w*, 988*m*. ^{1}H-NMR (500 MHz, $CDCl_3$): 9.95 (*s*, 1 H); 9.20 (*d*, *J* = 4.4, 2 H); 8.89 (*d*, *J* = 4.4, 2 H); 8.77 (*m*, 4 H); 7.68 (*t*, *J* = 8.5, 2 H); 7.22 (br. *s*, 2 H); 7.02 (*d*, *J* = 8.5, 4 H); 5.88 (br. *s*, 2 H); 4.08 (*t*, *J* = 6.8, 4 H); 3.82–3.98 (*m*, 8 H); 3.45–3.71 (*m*, 8 H); 3.21 (br. *s*, 4 H); 2.35 (*s*, 3 H); 1.72 (*t*, *J* = 6.8, 4 H); 1.05–1.48 (*m*, 28 H); 0.88 (*t*, *J* = 7.0, 4 H); 0.78 (*t*, *J* = 7.1, 12 H). ^{1}H-NMR (500 MHz, (D_5)pyridine): 10.15 (*s*, 1 H); 9.42 (*d*, *J* = 4.5, 2 H); 9.31 (*d*, *J* = 4.5, 2 H); 9.30 (*d*, *J* = 4.5, 2 H); 9.27 (*d*, *J* = 4.5, 2 H); 7.89 (*t*, *J* = 8.5, 2 H); 7.70 (*s*, 2 H); 7.62 (*s*, 2 H); 7.28 (*d*, *J* = 8.5, 4 H); 7.24 (*s*, 2 H); 7.10 (*s*, 2 H); 4.02–4.12 (*m*, 8 H); 3.99 (*t*, *J* = 6.3, 4 H); 3.84 (*t*, *J* = 7.2, 4 H); 3.62–3.71 (*m*, 8 H); 2.68 (*s*, 3 H); 1.69–1.79 (*m*, 4 H); 1.53–1.65 (*m*, 12 H); 1.31–1.49 (*m*, 12 H); 1.14–1.22 (*m*, 4 H); 0.74 (*t*, *J* = 7.1, 12 H). ^{13}C-NMR (125 MHz, $CDCl_3$): 173.0; 160.0; 154.8; 150.3; 150.1; 149.5; 148.9; 142.5; 134.4; 131.4; 131.1; 130.8; 130.1; 129.5; 126.2; 122.8; 119.5; 117.0; 113.0; 112.1; 111.1; 105.9; 104.4; 67.5; 67.4; 59.6; 46.4; 30.2; 29.4; 28.0; 25.5; 24.8; 23.8; 13.6; 8.4. ^{13}C-NMR (125 MHz, (D_5)pyridine): 172.5; 160.3; 156.0; 151.1; 151.0; 142.8; 137.6; 132.0; 131.9; 131.8; 131.1; 130.5; 129.6; 122.3; 120.9; 119.3; 113.3; 113.3; 112.5; 106.1; 105.3; 68.4; 67.9; 59.9; 46.7; 31.3; 29.8; 29.5; 26.5; 25.9; 24.5; 13.9; 9.2; 2 signals not observable due to overlap with solvent signals. FAB-MS: 1468.3 (100, M^+). Anal. calc. for $C_{81}H_{94}N_8O_{14}Zn$ (1469.07): C 66.23, H 6.45, N 7.63; found: C 66.06, H 6.61, N 7.46.

*Tetraethyl 4,4′,4″,4‴-[10-(3,5-Bis{[6-(1*H*-imidazol-1-yl)hexyl]oxy}-4-methylphenyl)-21*H*,23*H*-porphine-5,15-diylbis(benzene-2,1,3-triyldioxy)]tetrakis[butanoate]* (**4**·2 H). A purple soln. of **4**·Zn (14.7 mg, 0.01 mmol) in $CHCl_3$ (2.5 ml) was degassed by 3 'freeze-pump-thaw' cycles and then treated dropwise at 0° with CF_3COOH (0.10 ml, 1.30 mmol). The resulting dark-green soln. was stirred at r.t. for 10 min, then degassed sat. aq. Na_2CO_3 soln. (4 ml) was added. The resulting two-phase system was shaken vigorously, and the colorless aq. phase was separated from the now brown-purple org. layer with a syringe fitted with a long, thin needle. The org. layer was washed in a similar fashion with degassed H_2O (3 × 3 ml) and then immediately subjected to FC under N_2 (SiO_2 (10 g); CH_2Cl_2 → CH_2Cl_2/MeOH 95:5). The product-containing fractions were concentrated to dryness *in vacuo* in the dark, and the residue was recrystallized under N_2 from $CHCl_3$/heptane at −20° to give **4**·2 H (11.0 mg, 78%), which, in the solid state, was stable towards light and air for a few h. Brown-purple powder. M.p. 71°. TLC (SiO_2; CH_2Cl_2/MeOH 95:5): R_f 0.09. UV/VIS ($CHCl_3$): 639 (1100), 584 (4900), 543 (4000), 509 (16200), 415 (432300), 400 (sh, 78400), 303 (12400). IR (KBr): 3433*s* (br.), 2922*m*, 2867*w*, 1728*s*, 1583*m*, 1507*w*, 1456*s*, 1411*w*, 1372*w*, 1339*w*, 1244*m*, 1172*m*, 1122*m*, 1089*s*, 1028*w*, 967*w*, 794*w*. ^{1}H-NMR (300 MHz, $CDCl_3$): 10.10 (*s*, 1 H); 9.26 (*d*, *J* = 4.7, 2 H); 8.83–8.88 (*m*, 4 H); 8.81 (*d*, *J* = 4.7, 2 H); 7.73 (*t*, *J* = 8.4, 2 H); 7.48 (*s*, 2 H); 7.45 (*s*, 2 H); 7.05 (*s*, 2 H); 7.04 (*d*, *J* = 8.4, 4 H); 6.90 (*s*, 2 H); 4.06 (*t*, *J* = 6.1, 4 H); 3.80–4.00 (*m*, 12 H); 3.50–3.70 (*m*, 8 H); 2.44 (*s*, 3 H); 1.74–1.90 (*m*, 8 H); 1.49–1.63 (*m*, 4 H); 1.18–1.47 (*m*, 20 H); 0.75 (*t*, *J* = 7.1, 12 H); −2.87 (*s*, 2 H). ^{13}C-NMR (75 MHz, $CDCl_3$): 173.1; 160.0; 155.9; 145.0–148.9 (4 br.); 141.3; 137.6; 129.7–131.7 (4 br.); 130.5; 129.6; 120.6; 119.9; 119.0; 114.1; 112.9; 111.8; 105.8; 104.0; 68.4; 67.6; 59.8; 47.0;

31.1; 29.7; 29.4; 26.5; 25.8; 23.9; 13.8; 8.6. FAB-MS: 1406.4 (100, MH$^+$). HR-FAB-MS: 1405.7123 (M^+, $C_{81}H_{96}N_8O_{14}^+$; calc. 1405.7124).

*(*OT-*6-13)-([Tetraethyl 4,4′,4″,4‴-[10-(3,5-bis[[6-(1*H*-imidazol-1-yl)hexyl]oxy}-4-methylphenyl)-21*H*,23*H*-porphine]-5,15-diylbis(benzene-2,1,3-triyldioxy)]tetrakis(butanoato)}(2−)-*N^{21},N^{22},N^{23}, N^{24},N^3,N$^{3'}$*)iron(III) Chloride* ([**4**·Fe^{III}]Cl). To a soln. of **4**·2 H (28.1 mg, 0.020 mmol) in abs. THF (5 ml) degassed by 3 'freeze-pump-thaw' cycles, 2,6-lutidine (11.6 µl, 0.200 mmol) was added, and the purple soln. was heated to reflux for 15 min. Anh. $FeCl_2$ (25.3 mg, 0.200 mmol) was added, and the mixture was heated to reflux for 2 h. The red-brown soln. was left to cool to r.t. and was then exposed to air for 30 min to achieve complete oxidation to the Fe^{III} complex. Direct CC of the entire mixture (Al_2O_3 (10 g); THF → THF/MeOH 60:40) provided a red-brown oil, which was dried under h.v. The crude product was dissolved in 5 ml of $CHCl_3$, treated with 1% HCl in $CHCl_3$ (20 ml), and stirred at r.t. for 5 min. The solvent was evaporated *in vacuo*, and the residue was taken up in abs. THF (10 ml). To the dark brown soln., 1,8-bis(dimethylamino)naphthalene (34.3 mg, 0.160 mmol) was added, upon which the color immediately changed from dark brown to red-brown. The mixture was stirred at r.t for 15 min and then concentrated to dryness *in vacuo*. The crude, oily product was purified by prep. GPC (*Sephadex LH-20*, MeOH), dried under h.v., and finally recrystallized from $CHCl_3$/heptane to provide, after drying under h.v., [**4**·Fe^{III}]Cl (19.4 mg, 65%). Red-brown, crystalline solid. M.p. 105°. TLC (Al_2O_3; THF/MeOH 60:40): R_f 0.34. UV/VIS ($CHCl_3$): 543 (7500), 416 (124100), 318 (20000). IR (KBr): 2933*m*, 2967*w*, 1729*s*, 1633*w*, 1583*m*, 1523*w*, 1519*w*, 1456*m*, 1417*w*, 1379*w*, 1340*w*, 1320*w*, 1302*w*, 1250*m*, 1178*m*, 1125*m*, 1098*s*, 1029*w*, 1000*w*, 997*w*, 956*w*, 860*w*, 840*w*, 800*w*, 777*w*, 740*w*, 718*w*, 661*w*, 628*w*. EPR ($CHCl_3$): $g_x = 1.557$; $g_y = 2.322$; $g_z = 2.890$. $\mu_{eff}^{25°}$ ($CDCl_3$): $2.19 \pm 0.05\ \mu_B$. FAB-MS: 1458.8 (100, [M − Cl]$^+$). Anal. calc. for $C_{81}H_{94}N_8O_{14}FeCl \cdot 3\ H_2O$ (1549.03): C 62.81, H 6.51, N 7.23; found: C 62.75, H 6.56, N 6.80.

To synthesize the reduced complex [**4**·Fe^{II}], a soln. of [**4**·Fe^{III}]Cl in $CHCl_3$ of appropriate concentration was degassed with 3 'freeze-pump-thaw' cycles and then mixed with half its volume of a freshly prepared 0.1M soln. of $Na_2S_2O_4$ in degassed H_2O, upon which its color changed from red-brown to orange-red. The two-phase system was vigorously stirred for 15 min, and then left standing for 30 min to allow for a complete phase separation. The org. layer containing the desired [**4**·Fe^{II}] was then transferred *via* canula into the Ar-flushed vessels required for the individual measurements, or concentrated and dried under h.v. Orange-red, amorphous solid. UV/VIS ($CHCl_3$): 558 (4700), 531 (12500), 425 (165200), 310 (37300). $\mu_{eff}^{25°}$ ($CDCl_3$): $< 0.50\ \mu_B$.

*(*OT-*6-12)-[{Tetraethyl 4,4′,4″,4‴-[21*H*,23*H*-Porphine-5,15-diylbis(benzene-2,1,3-triyldioxy)]tetrakis-(butanoato)}(2−)-*N^{21},N^{22},N^{23},N^{24}*][bis[1-methylimidazolato](0)-*N^3*]iron(III) Chloride* ([**7**·(*N*-MeIm)$_2$-Fe^{III}]Cl). A soln. of **7**·2 H (49.0 mg, 0.050 mmol) [9c] in abs. THF (10 ml) was degassed by 3 'freeze-pump-thaw' cycles, then 2,6-lutidine (25.0 µl, 0.200 mmol) was added, and the purple soln. was heated to reflux for 15 min. Anh. $FeCl_2$ (63.0 mg, 0.500 mmol) was added, and the mixture was heated to reflux for 2 h. The red-brown soln. was left to cool to r.t. and was then exposed to air for 30 min. CC of the entire mixture (Al_2O_3 (15 g); THF) provided a red-brown oil, which was dried under h.v. The resulting black oil was dissolved in Et_2O (20 ml), washed with 1M HCl (10 ml) and sat. aq. NaCl soln. (10 ml), dried ($MgSO_4$), and concentrated *in vacuo*. The remaining black solid was recrystallized from Et_2O/pentane and dried under h.v. to yield a black crystalline solid of [**7**·Fe^{III}Cl], which was taken up in CH_2Cl_2 (5 ml). The dark brown soln. was treated with *N*-MeIm (9.0 µl, 0.110 mmol) and stirred at r.t. for 4 h, leading to a color change to red-brown. The solvent was evaporated *in vacuo*, and the crude, oily product was crystallized from MeOH/Et_2O and dried under h.v. to give [**7**·(*N*-MeIm)$_2$Fe^{III}]Cl (43.1 mg, 69%). Red-brown needles. M.p. 135°. TLC (Al_2O_3; THF/MeOH 60:40): R_f 0.70. UV/VIS (0.1M *N*-MeIm in $CHCl_3$): 538 (8100), 409 (142500), 315 (21200). IR (KBr): 2958*w*, 2950*w*, 2878*w*, 1728*s*, 1633*w*, 1589*m*, 1540*w*, 1522*w*, 1456*m*, 1417*w*, 1378*w*, 1360*w*, 1317*w*, 1295*w*, 1250*m*, 1178*m*, 1094*s*, 1061*w*, 1022*w*, 1000*m*, 995*m*, 944*m*, 961*w*, 840*w*, 789*w*, 767*w*, 722*w*, 700*w*, 672*w*, 650*w*, 622*w*. EPR (0.1M *N*-MeIm in $CHCl_3$): $g_x = 1.542$; $g_y = 2.313$; $g_z = 2.914$. $\mu_{eff}^{25°}$ (0.1M *N*-MeIm in $CDCl_3$): $2.05 \pm 0.05\ \mu_B$. FAB-MS: 1036.5 (100, [M − (2 *N*-MeIm) − Cl]$^+$). Anal. calc. for $C_{64}H_{72}N_8O_{12}FeCl \cdot H_2O$ (1256.66): C 61.27, H 5.95, N 8.93; found: C 61.05, H 6.01, N 9.13.

To prepare the reduced complex [**7**·(*N*-MeIm)$_2$Fe^{II}], a soln. of [**7**·(*N*-MeIm)$_2$Fe^{III}]Cl in 0.1M *N*-MeIm in $CHCl_3$ of appropriate concentration was degassed with 3 'freeze-pump-thaw' cycles and then mixed with half its volume of a freshly prepared 0.1M soln. of $Na_2S_2O_4$ in degassed H_2O, upon which its color changed from red-brown to orange-red. The two-phase system was vigorously stirred for 15 min, and then left standing for 30 min to allow for a complete phase separation. The org. layer, containing the desired [**7**·(*N*-MeIm)$_2$Fe^{II}], was then transferred *via* canula into the Ar-flushed vessels required for the individual measurements, or concentrated and dried under h.v. Orange-red, amorphous solid. UV/VIS (0.1M *N*-MeIm in $CHCl_3$): 553 (4600), 526 (14700), 419 (205400), 310 (36000). $\mu_{eff}^{25°}$ (0.1M *N*-MeIm in $CDCl_3$): $< 0.50\ \mu_B$.

Benzyl N-*(Tris{[3-oxo-3-({tris[(3-{2-[2-(2-methoxyethoxy)ethoxy]ethoxy}-3-oxopropoxy)methyl]methyl}-amino)propoxy]methyl}methyl)carbamate* (**20**). A soln. of **19** [25] (0.169 g, 0.358 mmol), **17** [25] (1.250 g, 1.613 mmol), and BtOH (0.219 g, 1.613 mmol) in abs. THF (10 ml) was cooled to 0° in an ice bath, and DCC (0.332 g, 1.613 mmol) was added in one portion. The suspension was slowly left to warm to r.t. during 24 h. After 5 d, the mixture was filtered through a 2-cm layer of *Celite* and concentrated *in vacuo*. The residue was taken up in PhMe (25 ml) and filtered again through a 2-cm layer of *Celite*. Concentration *in vacuo* gave an oily, crude product, which was purified by prep. GPC (*Bio-Beads S-X1*; PhMe). After drying under h.v., the product was taken up in three portions of CH_2Cl_2, filtered through *Celite*, and reconcentrated again *in vacuo*. Drying under h.v. afforded **20** (0.569 g, 58%). Colorless, highly viscous oil. TLC (SiO_2; CH_2Cl_2/MeOH 95:5): R_f 0.34. IR ($CHCl_3$): 2878*m*, 1729*s*, 1668*m*, 1600*w*, 1517*w*, 1472*w*, 1456*w*, 1422*w*, 1350*w*, 1106*s*, 1039*w*, 622*w*. ^{1}H-NMR (300 MHz, $CDCl_3$): 7.24–7.37 (*m*, 5 H); 6.10 (*s*, 3 H); 5.61 (*s*, 1 H); 5.02 (*s*, 2 H); 4.18–4.25 (*m*, 18 H); 3.50–3.72 (*m*, 138 H); 3.37 (*s*, 27 H); 2.55 (*t*, J = 6.4, 18 H); 2.37 (*t*, J = 6.5, 6 H). ^{13}C-NMR (75 MHz, $CDCl_3$): 171.6; 171.1; 155.3; 137.0; 128.5; 128.1; 127.9; 71.9; 70.5; 70.5 (2×); 69.3; 69.1; 69.0; 67.5; 66.6; 65.9; 63.6; 59.7; 59.0; 58.8; 37.1; 34.6. MALDI-TOF-MS (10^{-5} M in CH_2Cl_2; matrix: 0.5M THA in EtOH and 0.1M ammonium citrate in H_2O): 2767.8 (27, $[M+Na]^+$; $C_{123}H_{218}N_4O_{62}Na$; calc. 2767.4), 2745.6 (100, MH^+, $C_{123}H_{219}N_4O_{62}$; calc. 2745.4). Anal. calc. for $C_{123}H_{218}N_4O_{62}\cdot CH_2Cl_2$ (2830.00): C 52.63, H 7.84, N 1.98; found: C 52.62, H 7.64, N 2.05.

Tris{[3-oxo-3-({tris[(3-{2-[2-(2-methoxyethoxy)ethoxy]ethoxy}-3-oxopropoxy)methyl]methyl}amino)propoxy]methyl}methanamine (**18**). A mixture of **20** (0.412 g, 0.150 mmol) and ammonium formate (0.047 g, 0.750 mmol) in EtOH (5 ml) was degassed by passing N_2 through for 10 min, then Pd/C (10%, 0.060 g) was added and the mixture heated to 40° for 6 h with a slow stream of N_2 passing through. After cooling to r.t., the black suspension was filtered through a 2-cm layer of *Celite*, and the *Celite* was washed with $CHCl_3$/AcOEt 50:50 (30 ml). The filtrate and washings were combined and washed with sat. aq. NaCl soln. (15 ml), dried ($MgSO_4$), and evaporated *in vacuo*. Drying under h.v. gave **18** (0.391 g, 98%). Colorless, highly viscous oil. TLC (SiO_2; CH_2Cl_2/MeOH/Et_3N 95:4:1): R_f 0.26. IR ($CHCl_3$): 3368*w*, 2878*m*, 1730*s*, 1668*m*, 1516*w*, 1470*w*, 1383*w*, 1328*w*, 1244*m*, 1111*s*, 1033*w*, 989*w*, 950*w*, 911*w*, 856*w*, 622*w*. ^{1}H-NMR (300 MHz, $CDCl_3$): 6.16 (*s*, 3 H); 4.20–4.26 (*m*, 18 H); 3.51–3.73 (*m*, 132 H); 3.37 (*s*, 27 H); 3.30 (br. *s*, 6 H); 2.57 (*t*, J = 6.4, 18 H); 2.41 (br. *t*, J = 6.1, 6 H); 1.78 (br. *s*, 2 H). ^{13}C-NMR (75 MHz, $CDCl_3$): 171.8; 171.4; 73.0; 72.1; 70.7; 70.7 (2×); 69.2 (2×); 67.7; 66.8; 63.7; 59.9; 59.1; 56.1; 37.4; 34.8. MALDI-TOF-MS (10^{-5} M in CH_2Cl_2; matrix: 0.5M THA in EtOH and 0.1M ammonium citrate in H_2O): 2634.2 (12, $[M+Na]^+$, $C_{115}H_{212}N_4O_{60}Na$; calc. 2633.4), 2611.5 (100, MH^+; $C_{115}H_{213}N_4O_{60}$; calc. 2611.4). Anal. calc. for $C_{115}H_{212}N_4O_{60}\cdot 0.5\ CHCl_3$ (2670.63): C 51.95, H 8.02, N 2.10; found: C 51.97, H 7.52, N 2.10.

*(*SP*-4-2)({Tetrakis{2-[2-(2-methoxyethoxy)ethoxy]ethyl} 4,4′,4″,4‴-[10-(3,5-Bis{[6-(1*H*-imidazol-1-yl)hexyl]oxy}-4-methylphenyl)-21*H*,23*H*-porphine-1,15-diylbis(benzene-2,1,3-triyldioxy)]tetrakis[butanamido]}(2−)-*N^{21},N^{22},N^{23},N^{24}*)zinc(II)* (**1**·Zn). Compound **15**·Zn was prepared from **4**·Zn (29.4 mg, 0.020 mmol) according to *GP 1*. The black-purple powder was immediately dissolved in abs. DMF (2 ml) and, after addition of **16** [24] (65.3 mg, 0.400 mmol), the mixture was cooled to 0° in an ice bath. HATU (30.4 mg, 0.080 mmol) and Et_3N (56.0 µl, 0.400 mmol) were added, and the soln. was stirred at 0° for 2 h. The ice bath was removed, and the mixture was stirred for 1 d at r.t. in the dark. The solvent was distilled off under h.v. at 40°, and the residue was taken up in CH_2Cl_2/MeOH 95:5 (10 ml) and purified by FC (SiO_2 (5 g); CH_2Cl_2/MeOH 95:5). The porphyrin fraction was concentrated *in vacuo* and dried under h.v. overnight. Further purification by prep. GPC (*Bio-Beads S-X1*; CH_2Cl_2) and drying under h.v. provided **1**·Zn (33.1 mg, 85%). Purple, amorphous solid. TLC (SiO_2; CH_2Cl_2/MeOH 90:10): R_f 0.21. UV/VIS ($CHCl_3$): 595 (3100), 558 (12800), 515 (2700), 458 (8600), 426 (350500), 404 (sh, 34600), 311 (17100). IR ($CHCl_3$): 3400*w*, 2933*m*, 2877*m*, 1660*m*, 1583*m*, 1522*m*, 1456*m*, 1414*w*, 1378*w*, 1350*w*, 1328*w*, 1300*w*, 1283*w*, 1128*s*, 1100*s*, 1022*w*, 989*m*, 950*w*, 850*s*, 622*m*. ^{1}H-NMR (500 MHz, (D_5)pyridine): 10.14 (*s*, 1 H); 9.43 (*d*, J = 4.4, 2 H); 9.33 (*d*, J = 4.4, 2 H); 9.25–9.29 (*m*, 4 H); 7.85 (*t*, J = 8.5, 2 H); 7.71 (*s*, 2 H); 7.51 (*s*, 2 H); 7.41 (*s*, 2 H); 7.28 (*d*, J = 8.5, 4 H); 7.10 (*s*, 2 H); 5.10 (br. *s*, 4 H); 4.07–4.17 (*m*, 8 H); 3.91 (*t*, J = 6.2, 4 H); 3.78 (*t*, J = 7.1, 4 H); 3.15–3.60 (*m*, 48 H); 3.15 (*s*, 12 H); 2.65 (*s*, 3 H); 1.43–1.80 (*m*, 24 H); 1.33–1.41 (*m*, 4 H); 1.12–1.19 (*m*, 4 H). ^{13}C-NMR (75 MHz, (D_5)pyridine): 172.4; 160.8; 156.4; 151.6; 151.6; 142.9; 138.0; 132.4 (2×); 132.3; 131.7; 130.9; 129.5; 122.3; 121.1; 119.9; 113.7; 113.3; 106.2; 105.5; 72.3; 70.8; 70.7; 70.5; 70.3; 68.6; 68.5; 58.7; 41.0; 39.4; 31.2; 31.3; 29.6; 26.5; 25.9; 25.4; 9.2; 2 signals not observable due to overlap with solvent signals, 1 signal not observed due to signal overlap. FAB-MS: 1937.5 (100, M^+; $C_{101}H_{138}N_{12}O_{22}Zn$; calc. 1936.9). MALDI-TOF-MS (10^{-5} M in CH_2Cl_2; matrix: 0.5M THA in EtOH and 0.1M ammonium citrate in H_2O): 1962.0 (34, $[M+Na]^+$; $C_{101}H_{138}N_{12}O_{22}NaZn$; calc. 1959.9), 1938.2 (100, M^+; $C_{101}H_{138}N_{12}O_{22}Zn$; calc. 1936.9).

*(*SP*-4-2)-({Tetrakis{2-[2-(2-methoxyethoxy)ethoxy]ethyl} 17,17′,17″,17‴-[10-(3,5-Bis{[6-(1*H*-imidazol-1-yl)hexyl]oxy}-4-methylphenyl)-21*H*,23*H*-porphine-1,15-diylbis{benzene-2,1,3-triylbis[oxy(1-oxobutane-4,1-diyl)-*

imino]}]tetrakis[12-oxo-17-(5-oxo-2,6,9,12,15-pentaoxahexadec-1-yl)-2,5,8,11,15,19-hexaoxadocosan-22-ato]}(2 –)-N^{21},N^{21},N^{23},N^{24}*)zinc(II)* (**2**·Zn). Compound **15**·Zn was prepared from **4**·Zn (29.4 mg, 0.020 mmol) according to *GP 1*. The black-purple powder was immediately dissolved in abs. DMF (2 ml) and, after addition of **17** (124.0 mg, 0.160 mmol), the mixture was cooled to 0° in an ice bath. HATU (30.4 mg, 0.080 mmol) and Et_3N (21.2 µl, 0.160 mmol) were added, and the soln. was stirred at 0° for 2 h. The ice bath was removed, and the mixture was stirred for 3 d at r.t. in the dark. The solvent was distilled off under h.v. at 40°, and the residue was taken up in CH_2Cl_2/MeOH 95:5 (10 ml) and purified by FC (SiO_2 (5 g); CH_2Cl_2/MeOH 95:5). The porphyrin fraction was concentrated *in vacuo* and dried under h.v. overnight. Further purification by prep. GPC (*Bio-Beads S-X1*; CH_2Cl_2) and drying under h.v. gave **2**·Zn (56.8 mg, 65%). Purple, viscous oil. TLC (SiO_2; CH_2Cl_2/MeOH 90:10): R_f 0.31. UV/VIS ($CHCl_3$): 597 (4400), 560 (15600), 522 (3500), 427 (412100), 405 (sh, 45600), 312 (20800). IR ($CHCl_3$): 3411*w*, 2922*m*, 2877*m*, 1733*s*, 1668*m*, 1583*w*, 1522*w*, 1456*m*, 1377*w*, 1350*w*, 1322*w*, 1278*w*, 1250*m*, 1183*m*, 1106*s*, 1028*w*, 989*w*, 950*w*, 850*m*, 622*w*. ^{1}H-NMR (500 MHz, (D_5)pyridine): 10.25 (*s*, 1 H); 9.51 (*d*, *J* = 4.4, 2 H); 9.30–9.35 (*m*, 4 H); 9.26 (*d*, *J* = 4.4, 2 H); 7.95 (*t*, *J* = 8.5, 2 H); 7.86 (*s*, 2 H); 7.51 (*s*, 2 H); 7.40 (*d*, *J* = 8.5, 4 H); 7.27 (*s*, 2 H); 7.17 (*s*, 2 H); 5.44 (br. *s*, 4 H); 4.33 (*t*, *J* = 6.2, 4 H); 4.27–4.30 (*m*, 28 H); 4.09–4.21 (*m*, 8 H); 3.43–3.98 (*m*, 168 H); 3.25 (*s*, 36 H); 2.65 (*s*, 3 H); 2.62 (*t*, *J* = 6.3, 24 H); 1.82–2.00 (*m*, 8 H); 1.40–1.79 (*m*, 20 H); 1.16–1.23 (*m*, 4 H). ^{13}C-NMR (75 MHz, (D_5)pyridine): 172.9; 172.1; 160.9; 156.3; 151.5 (2×); 150.4; 150.4; 143.1; 137.7; 132.4 (3×); 131.6; 130.8; 128.7; 122.4; 121.0; 120.1; 113.5; 113.4; 113.2; 106.3; 105.6; 72.4; 71.0; 71.0; 70.9; 69.7; 69.4; 68.6; 67.3; 64.1; 60.6; 58.8; 47.3; 35.3; 32.3; 31.3; 29.6; 26.6; 26.0; 25.3; 9.2; 1 signal not observed due to signal overlap. MALDI-TOF-MS (10^{-5} M in CH_2Cl_2; matrix: 0.5M THA in EtOH and 0.1M ammonium citrate in H_2O): 4411.5 (28, $[M + Na]^+$, $C_{208}H_{330}N_{12}O_{82}ZnNa$; calc. 4411.1), 4388.6 (100, M^+; $C_{208}H_{330}N_{12}O_{82}Zn$; calc. 4388.1).

*(*SP*-4-2)-({Octakis[2-[2-(2-methoxyethoxy)ethoxy]ethyl} 13,13′,13″,13‴-[10-(3,5-Bis{[6-(1*H*-imidazol-1-yl)hexyl]oxy}-4-methylphenyl)-21*H*,23*H*-porphine-1,15-diylbis{benzene-2,1,3-triylbis[oxy(1-oxobutane-4,1-diyl)-imino]}]tetrakis[13-[5,12-dioxo-7,7-bis(5-oxo-2,6,9,12,15-pentaoxahexadec-1-yl)-2,9,13,16,19,22-hexaoxa-6-aza-tricos-1-yl]-8,18-dioxo-6,6,20,20-tetrakis(5-oxo-2,6,9,12,15-pentaoxahexadec-1-yl)-4,11,15,22-tetraoxa-7,19-diazapentacosanedioato}](2 –)*-N^{21},N^{22},N^{23},N^{24}*)zinc(II)* (**3**·Zn). Compound **15**·Zn was prepared from **4**·Zn (29.4 mg, 0.020 mmol) according to *GP 1*. The black-purple powder was immediately mixed with a soln. of **18** (627.0 mg, 0.240 mmol) in abs. PhMe (3 ml), and the mixture was concentrated to dryness *in vacuo* and further dried azeotropically by co-evaporation with abs. PhMe (3 × 3 ml). The heterogeneous mixture was dissolved in abs. DMF (2 ml) and cooled to 0° in an ice bath. HATU (45.6 mg, 0.120 mmol) and Et_3N (31.8 µl, 0.240 mmol) were subsequently added, and the soln. was stirred at 0° overnight, then allowed to very slowly warm to r.t. during 5 d. After stirring at r.t. for an additional 2 d, the solvent was distilled off under h.v. at 40°, and the residue was taken up in CH_2Cl_2/MeOH 95:5 (10 ml) and purified by FC (SiO_2 (5 g); CH_2Cl_2/MeOH 95:5). The porphyrin fraction was concentrated *in vacuo* and dried under h.v. overnight. Further purification was performed by prep. GPC (*Bio-Beads S-X1*; CH_2Cl_2), filtration through a poly(tetrafluoroethylene) (PTFE) membrane (∅ = 13 mm, pore size 0.45 µm), and prep. HP-GPC (*NovoGROM* 100, THF, 15 mg of mixture per run). Finally, the combined product was again purified by prep. GPC (*Bio-Beads S-X1*; CH_2Cl_2) and dried under h.v. to yield **3**·Zn (98.5 mg, 42%). Purple, highly viscous oil. TLC (SiO_2; CH_2Cl_2/MeOH 90:10): R_f 0.48. UV/VIS ($CHCl_3$): 595 (5100), 559 (20700), 520 (4200), 427 (544900), 408 (sh, 63600), 311 (22500). IR ($CHCl_3$): 3411*w*, 2920*m*, 2880*m*, 1734*s*, 1670*m*, 1579*vw*, 1520*m*, 1457*m*, 1380*w*, 1350*w*, 1323*w*, 1280*w*, 1245*m*, 1186*s*, 1108*s*, 1031*w*, 990*w*, 949*w*, 853*m*, 812*w*, 622*w*. ^{1}H-NMR (500 MHz, (D_5)pyridine): 10.20 (*s*, 1 H); 9.47 (*d*, *J* = 4.0, 2 H); 9.28–9.32 (*m*, 4 H); 9.23 (*d*, *J* = 4.0, 2 H); 8.05 (br. *s*, 2 H); 8.02 (*t*, *J* = 7.9, 2 H); 7.52 (*s*, 2 H); 7.49 (*d*, *J* = 7.9, 4 H); 7.40 (br. *s*, 2 H); 7.31 (br. *s*, 2 H); 6.30 (br. *s*, 16 H); 4.48–4.52 (*m*, 4 H); 4.41–4.45 (*m*, 4 H); 4.32–4.40 (*m*, 72 H); 4.10–4.22 (*m*, 8 H); 3.47–4.05 (*m*, 576 H); 3.29 (*s*, 108 H); 2.62 (*t*, *J* = 6.2, 72 H); 2.67 (*s*, 3 H); 1.55–1.73 (*m*, 24 H); 1.42–1.51 (*m*, 4 H); 1.21–1.32 (*m*, 4 H). ^{13}C-NMR (75 MHz, (D_5)pyridine): 172.4; 171.7; 171.4; 160.6; 155.9; 151.3; 151.2; 150.3; 150.2; 142.8; 136.7; 132.0 (2×), 131.9; 131.4; 130.7; 128.3; 122.1; 120.6; 120.3; 113.2; 113.1; 113.0; 106.1; 105.3; 72.5; 70.8; 70.8; 70.2; 69.7; 69.7; 69.3; 68.7; 68.4; 68.2; 67.3; 64.0; 60.6; 60.6; 58.7; 47.4; 37.3; 35.2; 32.1; 31.1; 29.4; 26.4; 25.9; 24.9. MALDI-TOF-MS (10^{-5} M in CH_2Cl_2; matrix: 0.01M HABA in MeCN/H_2O 1:1): 11750.8 (100, $[M + Na]^+$, $C_{533}H_{918}N_{24}O_{250}ZnNa$; calc. 11750.9), 11729.5 (37, M^+, $C_{533}H_{918}N_{24}O_{250}Zn$; calc. 11727.9).

*(*OT*-6-13)-({Tetrakis[2-[2-(2-methoxyethoxy)ethoxy]ethyl} 4,4′,4″,4‴-[10-(3,5-Bis{[6-(1*H*-imidazol-1-yl)-hexyl]oxy}-4-methylphenyl)-21*H*,23*H*-porphine-1,15-diylbis(benzene-2,1,3-triyldioxy)]tetrakis[butanamido]}-(2 –)*-N^{21},N^{22},N^{23},N^{24},N^{3},N$^{3'}$*)iron(III) Chloride* ([**1**·Fe^{III}]Cl). Compound [**1**·Fe^{III}]Cl (20.1 mg, 68%) was prepared from **1**·Zn (29.1 mg, 0.015 mmol) according to *GP 2*. The reaction time in the metal-insertion step was 2 h. Red-brown, amorphous solid. TLC (SiO_2; CH_2Cl_2/MeOH 90:10): R_f 0.10. UV/VIS ($CHCl_3$): 542 (8200), 415 (129200), 314 (21400). UV/VIS (H_2O): *Soret* band: 416 (54100); absorption at the *Soret* band of the

reduced complex: 428 (33500). IR ($CHCl_3$): 2928*s*, 2956*s*, 1670*s*, 1584*m*, 1520*m*, 1458*s*, 1415*w*, 1378*m*, 1349*w*, 1287*m*, 1261*s*, 1128*s*, 1101*s*, 1015*m*, 1004*m*, 954*w*, 851*w*, 808*w*, 620*w*. EPR ($CHCl_3$): $g_x = 1.557$; $g_y = 2.320$; $g_z = 2.894$. FAB-MS: 1928.0 (100, $[M - Cl]^+$, $C_{101}H_{138}N_{12}O_{22}Fe$; calc. 1927.9). MALDI-TOF-MS (10^{-5} M in CH_2Cl_2; matrix: 0.5M THA in EtOH and 0.1M ammonium citrate in H_2O): 1951.2 (30, $[M - Cl + Na]^+$, $C_{101}H_{138}N_{12}O_{22}FeNa$; calc. 1950.9), 1928.4 (100, $[M - Cl]^+$, $C_{101}H_{138}N_{12}O_{22}Fe$; calc. 1927.9).

The reduced Fe^{II} porphyrin dendrimer [**1**·Fe^{II}] was prepared *in situ* from [**1**·Fe^{III}]Cl according to *GP 3*. The reaction time for the reduction was 30 s. UV/VIS (H_2O): 558 (3200), 530 (9900), 428 (67000, *Soret* band); absorption at the *Soret* band of the oxidized complex: 416 (31300).

*(*OT-*6-13)-({Tetrakis[2-[2-(2-methoxyethoxy)ethoxy]ethyl} 17,17′,17″,17‴-[10-(3,5-Bis{[6-(1*H*-imidazol-1-yl)hexyl]oxy}-4-methylphenyl)-21*H*,23*H*-porphine-1,15-diylbis{benzene-2,1,3-triylbis[oxy(1-oxobutane-4,1-diyl)-imino]}]tetrakis[12-oxo-17-(5-oxo-2,6,9,12,15-pentaoxahexadec-1-yl)-2,5,8,11,15,19-hexaoxadocosan-22-ato]}(2 −)*-N^{21},N^{22},N^{23},N^{24})iron(III) Chloride ([**2**·Fe^{III}]Cl). Compound [**2**·Fe^{III}]Cl (32.3 mg, 73%) was prepared from **2**·Zn (43.9 mg, 0.010 mmol) according to *GP 2*. The reaction time in the metal insertion step was 4 h. Red-brown, viscous oil. TLC (SiO_2; CH_2Cl_2/MeOH 90:10): R_f 0.20. UV/VIS ($CHCl_3$): 542 (8800), 415 (131000), 297 (48800). UV/VIS (H_2O): *Soret* band: 416 (120400); absorption at the *Soret* band of the reduced complex: 425 (85900). IR ($CHCl_3$): 2927*s*, 2872*s*, 1732*s*, 1672*m*, 1585*w*, 1533*w*, 1512*w*, 1482*w*, 1458*m*, 1400*w*, 1374*m*, 1349*m*, 1323*w*, 1283*m*, 1261*m*, 1174*s*, 1105*s*, 1021*w*, 1004*m*, 954*w*, 861*w*, 611*w*. EPR ($CHCl_3$): $g_x = 1.555$; $g_y = 2.312$; $g_z = 2.881$. MALDI-TOF-MS (10^{-5} M in CH_2Cl_2; matrix: 0.01M HABA in MeCN/H_2O 1:1): 4402.2 (10, $[M - Cl + Na]^+$, $C_{209}H_{330}N_{12}O_{82}FeNa$; calc. 4401.1), 4379.3 (100, $[M - Cl]^+$, $C_{209}H_{330}N_{12}O_{82}Fe$; calc. 4378.1). The reduced Fe^{II} porphyrin dendrimer [**2**·Fe^{II}] was prepared *in situ* from [**2**·Fe^{III}]Cl according to *GP 3*. The reaction time for the reduction was 60 s. UV/VIS (H_2O): 559 (4900), 531 (13600), 425 (186500, *Soret* band); absorption at the *Soret* band of the oxidized complex: 416 (96500).

*(*OT-*6-13)-({Octakis[2-[2-(2-methoxyethoxy)ethoxy]ethyl} 13,13′,13″,13‴-[10-(3,5-Bis{[6-(1*H*-imidazol-1-yl)hexyl]oxy}-4-methylphenyl)-21*H*,23*H*-porphine-1,15-diylbis{benzene-2,1,3-triylbis[oxy(1-oxobutane-4,1-diyl)-imino]}]tetrakis{13-[5,12-dioxo-7,7-bis(5-oxo-2,6,9,12,15-pentaoxahexadec-1-yl)-2,9,13,16,19,22-hexaoxa-6-azatricos-1-yl]-8,18-dioxo-6,6,20,20-tetrakis(5-oxo-2,6,9,12,15-pentaoxahexadec-1-yl)-4,11,15,22-tetraoxa-7,19-diazapentacosanedioato}}(2 −)*-N^{21},N^{22},N^{23},N^{24},N^{3},$N^{3'}$)*iron(III) Chloride* ([**3**·Fe^{III}]Cl). Compound [**3**·Fe^{III}]Cl (69.2 mg, 78%) was prepared from **3**·Zn (88.1 mg, 0.0075 mmol) according to *GP 2*. The reaction time in the metal-insertion step was 6 h. Red-brown, highly viscous oil. TLC (SiO_2; CH_2Cl_2/MeOH 90:10) R_f 0.32. UV/VIS ($CHCl_3$): 543 (10200), 415 (128000), 313 (25400). UV/VIS (H_2O): *Soret* band: 416 (119500); absorption at the *Soret* band of the reduced complex: 424 (81800). IR ($CHCl_3$): 2916*s*, 2880*s*, 1734*s*, 1670*m*, 1578*w*, 1516*m*, 1458*m*, 1378*w*, 1350*w*, 1322*w*, 1239*m*, 1183*s*, 1109*s*, 1029*w*, 994*w*, 950*w*, 850*w*, 622*w*. EPR ($CHCl_3$): $g_x = 1.558$; $g_y = 2.321$; $g_z = 2.890$. MALDI-TOF-MS (10^{-5} M in CH_2Cl_2; matrix: 0.01M HABA in MeCN/H_2O 1:1): 11742.3 (12, $[M - Cl + Na]^+$, $C_{533}H_{918}N_{24}O_{250}FeNa$; calc. 11741.9), 11719.2 (100, $[M - Cl]^+$, $C_{533}H_{918}N_{24}O_{250}Fe$; calc. 11718.9). The reduced Fe^{II} porphyrin dendrimer [**3**·Fe^{II}] was prepared *in situ* from [**3**·Fe^{III}]Cl according to *GP 3*. The reaction time for the reduction was 90 s. UV/VIS (H_2O): 559 (4800), 531 (12900), 424 (176400, *Soret* band); absorption at the *Soret* band of the oxidized complex: 416 (96200).

Molecular Modeling. The modeling of a simple Fe^{II} tri(*meso*-phenyl)porphyrin to determine the optimal spacer length between porphyrin and imidazole ligand was performed with the UFF force field implemented in *Cerius*^{2} [14]. Low-energy conformations were obtained from high-temperature-quenched molecular dynamics and steepest-descent, followed by conjugate-gradient minimization at regular intervals along the simulation trajectory. Structures were scored by calculating the energetic difference between the complexed and the non-complexed forms, which had to be as negative as possible, as it corresponds to the complexation energy of the ligand to the metal center. Linker lengths of six and more CH_2 units gave almost identical complexation energies. A linker with five CH_2 units gave a slightly less favorable complexation energy, and still shorter linkers led to a large energetic penalty upon complexation due to the build up of large amounts of strain energy. The complexation energy was strongly positive in the cases of three and four CH_2 units in the linker moiety.

The model of the second-generation dendrimer (*Fig. 2*) was obtained by energy minimization of a randomly drawn starting structure with *Insight II, V. 2.3*, *BIOSYM Technologies, Inc.*, San Diego, CA, 1993, as described in [9c]. The geometry of the core was fully restrained to its minimized structure, which was obtained from a molecular-dynamics conformational search as described above. The Fe-atom was replaced with a dummy atom to carry out the energy minimization due to the nonavailability of suitable force-field parameters in *Insight II*.

Electrochemical Experiments. The measurements were performed under Ar in dry, carefully degassed MeCN or CH_2Cl_2 (5.00 ml) containing 0.1M Bu_4NPF_6, typically with 0.5 mM solns. of porphyrin at 298 ± 2 K. A glassy C mini-electrode was used as the working electrode, a Ag/AgCl electrode from *Bioanalytical Systems* was

used as the reference, and 0.5 mM ferrocene (Fc) was added as an internal potential standard. A Pt wire served as the counter-electrode. A typical scan was run at a rate of 100 mV s^{-1}, and no soln. resistance compensation was applied.

Spectroelectrochemical measurements were conducted in a custom-made borosilicate glass cell with an optical-path length of 0.1 mm on an OTTLE (optically transparent thin-layer electrode). A Pt grid (1000 mesh) positioned in the optical path was used as the working electrode; reference and counter-electrodes were as indicated above. The cell was placed in an *Hewlett-Packard 8453* diode-array spectrophotometer, and UV/VIS spectra were recorded during electrolysis. An *EG & G Princeton Applied Research* model *263A Potentiostat/Galvanostat* (cyclic voltammetry (CV)) or an *Autolab-EcoChemie Multipurpose Electrochemical Device* (CV and steady-state voltammetry (SSV) and spectroelectrochemistry) were used to obtain the measurements. All the redox potentials were determined with Fc as an internal standard, and the redox potentials were subsequently referenced against the standard calomel electrode (SCE) by means of published values for the Fc/Fc^+ couple in CH_2Cl_2 (0.46 V *vs.* SCE [27a]) and MeCN (0.45 V *vs.* SCE [27b]).

Equilibrium Measurements by Optical Spectroscopy. All experiments were conducted in the dark under Ar in septum-sealed quartz cuvettes, and all solns. were prepared with carefully degassed, distilled *MilliQ*-filtered H_2O. A stock soln. (1.00 ml) of fully oxidized porphyrin (typical concentration $5 \cdot 10^{-6}$ M) was titrated at 298 ± 2 K with a stock soln. of fully reduced reference compound (typical concentration $2.5 \cdot 10^{-4}$ M), and the concentrations of all species in soln. were calculated at each titration point from the spectrophotometrically determined ratio of oxidized to reduced porphyrin and the known total concentrations. As the total concentration of porphyrin complexes varies during the course of the titration experiment, isosbestic points are not observed. *Eqns. 1* and *2* derived from *Lambert-Beer*'s law at the *Soret* bands of the reduced (Fe^{II}) and oxidized (Fe^{III}) porphyrin complexes were used to determine the concentrations of reduced (c_{red}) and oxidized (c_{ox}) porphyrin complex spectrophotometrically.

$$c_{ox} = \frac{\varepsilon^{red}_{ox\,max} \cdot A_{red\,max} - \varepsilon^{red}_{red\,max} \cdot A_{ox\,max}}{\varepsilon^{ox}_{red\,max} \cdot \varepsilon^{red}_{ox\,max} - \varepsilon^{red}_{red\,max} \cdot \varepsilon^{ox}_{ox\,max}} \quad (1)$$

$$c_{red} = \frac{\varepsilon^{ox}_{ox\,max} \cdot A_{red\,max} - \varepsilon^{ox}_{red\,max} \cdot A_{red\,max}}{\varepsilon^{red}_{red\,max} \cdot \varepsilon^{ox}_{ox\,max} - \varepsilon^{ox}_{red\,max} \cdot \varepsilon^{red}_{ox\,max}} \quad (2)$$

c_{ox}: concentration of oxidized Fe^{III} porphyrin complex,

c_{red}: concentration of reduced Fe^{II} porphyrin complex,

$A_{ox\,max}$: absorption at the *Soret* band of the oxidized complex,

$A_{red\,max}$: absorption at the *Soret* band of the reduced complex,

$\varepsilon^{ox}_{ox\,max}$: molar extinction coefficient of the oxidized complex at its *Soret* band,

$\varepsilon^{ox}_{red\,max}$: molar extinction coefficient of the oxidized complex at the *Soret* band of the reduced complex,

$\varepsilon^{red}_{red\,max}$: molar extinction coefficient of the reduced complex at its *Soret* band,

$\varepsilon^{red}_{ox\,max}$: molar extinction coefficient of the reduced complex at the *Soret* band of the oxidized complex

E Values *vs.* the normal hydrogen electrode (NHE) were then obtained from a nonlinear least-squares fit of the data from the series of equilibria produced during the titration to the *Nernst* equation by means of the known standard reduction potentials of the reference compound and the concentrations of its oxidized and reduced forms, which were obtained as outlined above, to calculate the ambient reduction potential at each titration point. *E* Values were then referenced for comparison against SCE (0.24 V *vs.* NHE [27c]). Either $K_4[Fe(ox)_3]$ (prepared *in situ* from $[(NH_4)_2Fe(SO_4)_2 \cdot H_2O]$ in presence of 0.5M $K_2(ox)$: $E_{1/2} = +0.002$ V *vs.* NHE [28a,b]) or $K_4[Fe(CN)_6]$ ($E_{1/2} = +0.355$ V *vs.* NHE [28c,d]) were used as the reference compound. Titrations were reproduced with excellent agreement in triplicate runs.

REFERENCES

[1] G. R. Moore, G. W. Pettigrew, 'Cytochromes-c: Evolutionary, Structural and Physicochemical Aspects', Springer, Berlin, 1990; F. S. Mathews, *Prog. Biophys. Molec. Biol.* **1985**, *45*, 1.

[2] K. M. Kadish, M. M. Morrison, L. A. Constant, L. Dickens, D. G. Davis, *J. Am. Chem. Soc.* **1976**, *98*, 8387; A. Giraudeau, H. J. Callot, J. Jordan, I. Ezhar, M. Gross, *J. Am. Chem. Soc.* **1979**, *101*, 3857.

[3] a) H. A. Harbury, J. R. Cronin, M. W. Fanger, T. P. Hettinger, A. J. Murphy, Y. P. Myer, S. N. Vinogradov, *Proc. Natl. Acad. Sci. U.S.A.* **1965**, *54*, 1658; b) P. K. Warme, L. P. Hager, *Biochemistry* **1970**, *9*, 1606; c) J.-C. Marchon, T. Mashiko, C. A. Reed, in 'Electron Transport and Oxygen Utilization', Ed. C. Ho, Elsevier, North Holland, 1982, pp. 67–72; d) S. G. Sligar, K. D. Egeberg, J. T. Sage, D. Morikis, P. M. Champion, *J. Am. Chem. Soc.* **1987**, *109*, 7896; e) A. L. Raphael, H. B. Gray, *J. Am. Chem. Soc.* **1991**, *113*, 1038.

[4] R. Quinn, J. Mercer-Smith, J. N. Burstyn, J. S. Valentine, *J. Am. Chem. Soc.* **1984**, *106*, 4136; P. O'Brien, D. A. Sweigart, *Inorg. Chem.* **1985**, *24*, 1405.

[5] K. M. Barkigia, L. Chantranupong, K. M. Smith, J. Fajer, *J. Am. Chem. Soc.* **1988**, *110*, 7566; K. M. Kadish, E. van Caemelbecke, P. Boulas, F. D'Souza, E. Vogel, M. Kisters, C. J. Medforth, K. M. Smith, *Inorg. Chem.* **1993**, *32*, 4177.

[6] E. Stellwagen, *Nature* **1978**, *275*, 73; K. M. Kadish, L. A. Bottomley, S. Kelly, D. Schaeper, L. R. Shiue, *Bioelectrochem. Bioenerget.* **1981**, *8*, 213; L. A. Bottomley, K. M. Kadish, *Inorg. Chem.* **1981**, *20*, 1348.

[7] a) R. J. Kassner, *Proc. Natl. Acad. Sci. U.S.A.* **1972**, *69*, 2263; b) R. J. Kassner, *J. Am. Chem. Soc.* **1973**, *95*, 2674; A. K. Churg, A. Warshel, *Biochemistry* **1986**, *25*, 1675; D. Lexa, M. Momenteau, P. Rentien, G. Rytz, J.-M. Savéant, F. Xu, *J. Am. Chem. Soc.* **1984**, *106*, 4755; C. Gueutin, D. Lexa, M. Momenteau, J.-M. Savéant, F. Xu, *Inorg. Chem.* **1986**, *25*, 4294.

[8] M. S. Caffrey, M. A. Cusanovich, *Arch. Biochem. Biophys.* **1991**, *285*, 227; K. K. Rodgers, S. G. Sligar, *J. Am. Chem. Soc.* **1991**, *113*, 9419.

[9] a) P. J. Dandliker, F. Diederich, M. Gross, C. B. Knobler, A. Louati, E. M. Sanford, *Angew. Chem.* **1994**, *106*, 1821; *Angew. Chem., Int. Ed.* **1994**, *33*, 1739; b) P. J. Dandliker, F. Diederich, J.-P. Gisselbrecht, A. Louati, M. Gross, *Angew. Chem.* **1995**, *107*, 2906; *Angew. Chem., Int. Ed.* **1995**, *34*, 2725; c) P. J. Dandliker, F. Diederich, A. Zingg, J.-P. Gisselbrecht, M. Gross, A. Louati, E. Sanford, *Helv. Chim. Acta* **1997**, *80*, 1773.

[10] a) K. W. Pollak, J. W. Leon, J. M. J. Fréchet, M. Maskus, H. D. Abruña, *Chem. Mater.* **1998**, *10*, 30; b) D.-L. Jiang, T. Aida, *J. Am. Chem. Soc.* **1998**, *120*, 10895; c) P. Bhyrappa, G. Vaijayanthimala, K. S. Suslick, *J. Am. Chem. Soc.* **1999**, *121*, 262; d) S. A. Vinogradov, L.-W. Lo, D. F. Wilson, *Chem.–Eur. J.* **1999**, *5*, 1338; e) U. Puapaiboon, R. T. Taylor, *Rapid Commun. Mass Spectrom.* **1999**, *13*, 508; f) M. Kimura, T. Shiba, M. Yamazaki, K. Hanabusa, H. Shirai, N. Kobayashi, *J. Am. Chem. Soc.* **2001**, *123*, 3036.

[11] a) F. Zeng, S. C. Zimmerman, *Chem. Rev.* **1997**, 97, 1681; b) Y. Kim, S. C. Zimmerman, *Curr. Opin. Chem. Biol.* **1998**, *2*, 733; c) D. K. Smith, F. Diederich, *Chem.–Eur. J.* **1998**, *4*, 1353; d) H.-F. Chow, T. K.-K. Mong, M. F. Nongrum, C.-W. Wan, *Tetrahedron* **1998**, *54*, 8543; e) O. A. Matthews, A. N. Shipway, J. F. Stoddard, *Prog. Polym.* **1998**, *23*, 1; f) G. R. Newkome, E. He, C. N. Moorefield, *Chem. Rev.* **1999**, *99*, 1689; g) C. B. Gorman, J. C. Smith, *Acc. Chem. Res.* **2001**, *34*, 60.

[12] P. Weyermann, J.-P. Gisselbrecht, C. Boudon, F. Diederich, M. Gross, *Angew. Chem.* **1999**, *111*, 3400; *Angew. Chem., Int. Ed.* **1999**, *38*, 3215.

[13] a) F. S. Mathews, M. Levine, P. Argos, *Nature* **1971**, *233*, 15; b) S. F. Velick, P. Strittmatter, *J. Biol. Chem.* **1955**, *221*, 265.

[14] UFF force field implemented in *Cerius*^{2}, V. 3.0, *BIOSYM Technologies, Inc.*, San Diego, CA, 1997.

[15] a) R. Swanson, B. L. Trus, N. Mandel, G. Mandel, O. B. Kallai, R. E. Dickerson, *J. Biol. Chem.* **1977**, *252*, 759; b) F. L. Rodkey E. G. Ball, *J. Biol. Chem.* **1950**, *182*, 17.

[16] A. Suzuki, in 'Metal-Catalyzed Cross-coupling Reactions', Eds. F. Diederich, P. J. Stang, Wiley-VCH, 1997, pp. 49–97.

[17] F. P. Doyle, J. H. C. Nayler, H. R. J. Waddington, J. C. Hanson, G. R. Thomas, *J. Chem. Soc.* **1963**, 497.

[18] F. Montanari, M. Penso, S. Quici, P. Viganò, *J. Org. Chem.* **1985**, *50*, 4888.

[19] H. Kobayashi, T. Higuchi, Y. Kaizu, H. Osada, M. Aoki, *Bull. Chem. Soc. Jpn.* **1975**, *48*, 3137; F. A. Walker, M.-W. Lo, M. T. Ree, *J. Am. Chem. Soc.* **1976**, *98*, 5552.

[20] J. Peisach, W. E. Blumberg, A. Adler, *Ann. N. Y. Acad. Sci.* **1973**, *206*, 310; G. N. La Mar, F. A. Walker, *J. Am. Chem. Soc.* **1973**, *95*, 1782; R. Quinn, M. Nappa, J. S. Valentine, *J. Am. Chem. Soc.* **1982**, *104*, 2588.

[21] L. M. Epstein, D. K. Straub, C. Maricondi, *Inorg. Chem.* **1967**, *6*, 1720; K. M. Adams, P. G. Rasmussen, W. R. Scheidt, K. Hatano, *Inorg. Chem.* **1979**, *18*, 1892.

[22] D. F. Evans, *J. Chem. Soc.* **1959**, 2003; J. Löliger, R. Scheffold, *J. Chem. Educ.* **1972**, *49*, 646.

[23] H. Kobayashi, M. Shimizu, I. Fujita, *Bull. Chem. Soc. Jpn.* **1970**, *43*, 2335; H. Kobayashi, Y. Yanagawa, *Bull. Chem. Soc. Jpn.* **1972**, *45*, 450.

[24] M. Schmidt, R. Amstutz, G. Crass, D. Seebach, *Chem. Ber.* **1980**, *113*, 1691.

[25] T. Habicher, F. Diederich, V. Gramlich, *Helv. Chim. Acta* **1999**, *82*, 1066.

[26] L. A. Constant, D. G. Davis, *Anal. Chem.* **1975**, *47*, 2253; K. M. Kadish, L. A. Bottomley, *Inorg. Chem.* **1980**, *19*, 832; M. J. M. Nesset, N. V. Shokhirev, P. D. Enemark, S. E. Jacobsen, F. A. Walker, *Inorg. Chem.* **1996**, *35*, 5188.

[27] a) N. G. Connely, W. E. Geiger, *Chem. Rev.* **1996**, *96*, 877; b) W. G. Barette Jr., H. W. Johnson Jr., D. T. Sawyer, *Anal. Chem.* **1984**, *56*, 1890; c) D. T. Sawyer, A. Sobkowiak, J. L. Roberts, 'Electrochemistry for Chemists', 2nd edn., John Wiley & Sons, New York, 1995, Chapt. 5, pp. 170–248.

[28] a) J. J. Lingane, *J. Am. Chem. Soc.* **1946**, *68*, 2448; b) W. B. Schaap, H. A. Laitinen, J. C. Bailar Jr., *J. Am. Chem. Soc.* **1954**, *76*, 5868; c) R. C. Murray Jr., P. A. Rock, *Electrochim. Acta* **1968**, *13*, 969; d) G. I. H. Hanania, D. H. Irvine, W. A. Eaton, P. George, *J. Phys. Chem.* **1967**, *71*, 2022.

[29] L. P. Dutton, *Methods Enzymol.* **1978**, *54*, 411.

[30] S. Serroni, S. Campagna, A. Juris, M. Venturi, V. Balzani, G. Dendti, *Gazz. Chim. Ital.* **1994**, *124*, 423; G. R. Newkome, R. Güther, C. N. Moorefield, F. Cardullo, L. Echegoyen, E. Pérez-Cordero, H. Luftmann, *Angew. Chem.* **1995**, *107*, 2159; *Angew. Chem., Int. Ed.* **1995**, *34*, 2023; H. F. Chow, I. Y.-K. Chan, D. T. W. Chan, R. W. M. Kwok, *Chem.–Eur. J.* **1996**, *2*, 1085; C. B. Gorman, J. C. Smith, M. W. Hager, B. L. Parkhurst, H. Sierzputowska-Gracz, C. A. Haney, *J. Am. Chem. Soc.* **1999**, *121*, 9958; G. R. Newkome, V. V. Narayanan, L. Echegoyen, E. Pérez-Cordero, H. Luftmann, *Macromolecules* **1997**, *30*, 5187; C. M. Cardona, T. Donovan McCarley, A. E. Kaifer, *J. Org. Chem.* **2000**, *65*, 1857; D. K. Smith, *J. Chem. Soc., Perkin Trans. 2* **1999**, 1563; G. R. Newkome, A. K. Patri, L. A. Godínez, *Chem. – Eur. J.* **1999**, *5*, 1445; F. Vögtle, M. Plevoets, M. Nieger, G. C. Azzellini, A. Credi, L. De Cola, V. De Marchis, M. Venturi, V. Balzani, *J. Am. Chem. Soc.* **1999**, *121*, 6290; M. Kimura, T. Shiba, T. Muto, K. Hanabusa, H. Shirai, *Chem. Commun.* **2000**, 11; S. Mondal, P. Basu, *Inorg. Chem.* **2001**, *40*, 192; T. Liwporncharoenvong, R. L. Luck, *J. Am. Chem. Soc.* **2001**, *123*, 3615.

[31] S. De Backer, Y. Prinzie, W. Verheijen, M. Smet, K. Desmedt, W. Dehaen, F. C. De Schryver, *J. Phys. Chem. A* **1998**, *102*, 5451.

Received September 4, 2001